RESEARCH ARTICLE-MECHANICAL ENGINEERING

A New Saturated Two-Phase Flow Boiling Correlation Based on Propane (R290) Data

Oguz Emrah Turgut[1] · Mustafa Turhan Coban[2]

Abstract

There are plenty of literature research studies investigating two-phase heat transfer characteristics of propane under varying operational conditions. Based on the collected data retrieved from the experimental measurements, several flow boiling heat transfer correlations have been proposed up to now. However, the prediction accuracy of the proposed correlations for propane refrigerant is still in question as most of the correlation is developed for their measurements or derived for a limited range of operational conditions. To conquer this drawback, this study proposes a new flow boiling heat transfer model for smooth tubes based on a propane experimental database compiled of 2179 points obtained from different eighteen laboratories around the world. Operational conditions of the database cover mass fluxes between 50 and 600 kg/m^{2}s, saturation temperatures between -35.0 and 43.0 °C, heat fluxes between 2.5 and 227.0 kW/m^2, hydraulic diameters between 0.3 and 7.7 mm, and thermodynamic qualities 0.01 to 0.99. Estimations performed by the new flow boiling model have been compared to those obtained by the literature correlations, and comparative results indicate that the proposed model surpasses the existing flow boiling in terms of prediction accuracy with a mean absolute error of 19.1% and mean relative error of 1.7%.

List of Symbols

Bd — Bond number

Bo — Boiling number, $\mathrm{Bo} = \frac{Q}{G \cdot h_{\mathrm{fg}}}$

C — Chisholm parameter

C_n — Correlation constant

Co — Convection number, $\mathrm{Co} = \left(\frac{1-x}{x}\right)^{0.8}\left(\frac{\rho_v}{\rho_l}\right)^{0.5}$

Conf — Confinement number, $\mathrm{Conf} = \frac{\sqrt{\left(\frac{\sigma}{g(\rho_l - \rho_v)}\right)}}{D_h}$

Cp — Specific heat capacity (kJ/kg K)

D_h — Hydraulic tube diameter (m)

f — Friction factor

F — Two phase multiplier

Fr — Froude number, $\mathrm{Fr} = \frac{G^2}{g \cdot D_h \cdot \rho^2}$

F_f — Fluid specific constant for Kandlikar correlation

g — Gravitational acceleration constant (m/s^2)

G — Mass flux (kg/m^{2}s)

h — Heat transfer coefficient (W/m^{2}K)

h_{fg} — Latent heat of vaporization (kJ/kg)

k — Thermal conductivity (W/mK)

M — Molar mass (kg/kmol)

MAE — Mean absolute error

MRE — Mean relative error

N — Number of experimental data

p_r — Reduced pressure, $p_r = \frac{p_{\mathrm{sat}}}{p_{\mathrm{crit}}}$

Pr — Prandtl number, $\mathrm{Pr} = \frac{\mu \cdot c_p}{k}$

Q, q — Heat flux (W/m^2)

Re_l — Liquid Reynolds number, $\mathrm{Re}_l = \frac{G(1-x)D_h}{\mu_l}$

Re_{lo} — Liquid-only Reynolds number, $\mathrm{Re}_{lo} = \frac{G \cdot D_h}{\mu_l}$

S — Suppression factor

T — Temperature (°C/K)

x — Vapor quality

X_{tt} — Lockhart–Martinelli parameter, $X_{\mathrm{tt}} = \left(\frac{1-x}{x}\right)^{0.9}\left(\frac{\rho_v}{\rho_l}\right)^{0.5}\left(\frac{\mu_l}{\mu_v}\right)^{0.1}$

We — Weber number, $\mathrm{We} = \frac{G^2 \cdot g}{\rho \cdot \sigma}$

Greek symbols

ε — Surface roughness (μm)

μ — Dynamic viscosity (Pa s)

✉ Oguz Emrah Turgut
oeturgut@hotmail.com

[1] Industrial Engineering Department, Engineering and Architecture Faculty, Izmir Bakircay University, 35667 Menemen, Izmir, Turkey

[2] Mechanical Engineering Department, Ege University, 35040 Bornova, Izmir, Turkey

Springer

ρ	Density (kg/m^3)
σ	Surface tension (Pa/m

Subscripts

calc	Calculated
cb	Convective boiling
crit	Critical
exp	Experimental
g, V	Gas, vapor
l	Liquid
lo	Liquid only
nb	Nucleate boiling
pred	Predicted
sat	Saturated
sp	Single phase
tp	Two-phase

1 Introduction

Boiling in mini and microchannels along with their applications in different cooling industries has drawn significant interest among the heat transfer research community. Two-phase heat transfer occurring in the heat exchange equipment of a refrigeration system plays an important role in designing feasible and efficient heat exchange devices. Transferring the available heat from hot to cold medium in the manner of two-phase flow boiling rather than single-phase flow provides a more effective way based on the amount of heat transfer exchanged between the running streams. Practical outcomes of the industrial applications reveal that a phase change of refrigerant flowing in channels needs to be deeply investigated and the governing transport mechanism that drives the flow boiling process should be extensively analyzed to develop a sustainable and reliable mathematical model that predicts the total heat exchange rate between the hot and cold streams. Despite the prevalent utilization of the small scale mini and microdevices in the industry, there has been accomplished a limited amount of experimental and theoretical study in this hot spot research area. Some of the practical advantages of using flow boiling in small channels in heat exchange devices include providing a compact heat transfer surface and high heat transfer rates, minimizing the thermal resistance between the tube wall and stream, and entailing a low capital cost, etc. [1]. Furthermore, the flow boiling heat transfer process provides enhanced heat removal rates per unit volume and offers unique attributes such as compactness and temperature uniformity along the cooling channel which allows for its favorable utilization in the modern application areas ranging from avionics to laser industries.

The early 1980s witnessed two important events that accelerate the development of convective boiling heat transfer in channels [2]. Rapid advancements that occurred in the microchip technology during this period entail a huge heat dissipation to the ambient which nearly amounts to 1000 kW/m^2 heat flux rate. This significant increase in heat emission rates urged practitioners and researchers to innovate current technologies in cooling devices utilizing the merits of flow boiling heat transfer to maintain plausible and stable saturation temperatures of the units to be cooled. Another decisive event is the Montreal Protocol, which is devoted to protecting the ozone layer from the various types of ozone-depleting substances by phasing them out of production and utilization [3]. Awareness of the hazardous effects of CFCs and HCFCs on global warming as well as ozone depletion had been widely prevalent even before the advent of the Montreal Protocol. This international treaty restricts the production and usage of CFC- and HCFC-based refrigerants and a great deal of effort has been made up to now to procure replacement refrigerants for CFCs and HCFCs. Researchers have proposed novel refrigerants having different thermophysical characteristics to fill this gap, which gives rise to the production of an extensive number of refrigerant alternatives that boosts up the efforts on better understanding the thermal properties of the investigated refrigerants and focus the research activities on investigating essential features of the proposed alternative refrigerants to comprehend their underlying two-phase heat transfer mechanisms.

Research on HFC refrigerants has been the main issue since the imposed regulations proclaimed by the lawmakers and international organizations due to their widespread usage in different cooling applications. Notwithstanding that, HFC- and HCFC-based refrigerants have high Global Warming Potentials (GWP) despite having a negligible negative influence on the ozone layer [4]. These types of refrigerants are also known as greenhouse gases playing a vital role in contributing to climatic changes and environmental problems, which are some of the inevitable results of the global warming phenomenon. Two available options can be referred to minimize the detrimental effects of greenhouse gases on the environment. One option is using mini channel heat exchangers relying on their higher heat transfer rates and low fluid inventory [5]. Another option is to replace the ozone-depleting harmful HFCs with environmentally friendly natural refrigerants trusting on their relatively low GWP and ODP indexes. Among the available refrigerants proposed for the replacement alternatives, propane (R290) can be a plausible candidate thanks to its lower GWP rates (5), outstanding transport properties, and applicable material compatibilities. However, higher flammability and low ignition concentration of propane necessitate a proper optimization procedure for thermal design to maintain an optimum heat exchanger size for reducing the fluid charge. The latent heat of vaporization value of propane is nearly double of any

CFC- and HFC-based refrigerant which implicitly explains that half the mass flow rate requires to circulate the running process fluid throughout the thermal system in comparison with that of the CFCs and HCFCs for the same heat duty. James and Missenden [6] indicated that the flow charge of propane is so small and negligible which almost eliminates the possible risk of explosion as an unprecedented outcome of accidental leakages in household appliances. Propane shows a stable chemical behavior and complies with the most of materials and miscible fluids most of which are used as lubricants in a compressor. Besides, propane has a compatible thermophysical property with HFC-based refrigerants, which makes this refrigerant suitable for retrofitting. All these favorable features of propane make it attractive and worthwhile to be extensively investigated and studied. Therefore, many researchers made experimental and theoretical analyses particularly on flow boiling characteristics of propane in mini and microchannels.

Shin et al. [7] measured convective flow boiling heat transfer coefficients and pressure drop gradients of some pure refrigerants including propane and refrigerant mixtures and compared the experimental data with the predictive results obtained by Gungor and Winterton [8] correlation. It was observed that two-phase heat transfer coefficient rates are strongly dependent upon heat flux at lower qualities. Lee et al. [9] made an experimental study on flow boiling heat transfer characteristics and pressure drop gradients of some widely known hydrocarbon refrigerants of R290, R600, R1270, and HCFC-based refrigerant R22 inside a horizontal double pipe heat exchanger. Experimental results reveal that both the heat transfer coefficient and pressure drop values of hydrocarbon refrigerants are higher than that of R22. Wen and Ho [10] reported experimental results of two-phase flow boiling and pressure drop of R290, R600, and R90/R600 mixtures flowing in a three-line serpentine small tube bank. They proposed a novel flow boiling correlation based on the complied experimental data. Zou et al. [11] conducted experimental research studies on flow boiling characteristics of binary refrigerant mixtures of R290/R152a. Variational influences of mass flux, heat flux, saturation temperatures, and vapor qualities over heat transfer coefficient values were discussed and accuracies of the existing flow boiling correlations were analyzed. Maqbool et al. [5] carried out experimental research studies on flow boiling heat transfer and pressure drop of propane flowing in a vertical stainless-steel tube with 1.7 mm inner diameter and 245 mm heated length. Results showed that heat transfer rates are increased with increasing mass flux and vapor qualities and decreasing saturation pressures which are in line with the tendencies of other HCFC refrigerants. Yunos et al. [12] analyzed the contributions of two different flow boiling mechanisms including nucleate boiling and forced convection. They considered mass flux, heat flux, and vapor qualities as design variables to maximize the flow boiling heat transfer coefficient rates. Optimization results along with comparative analysis between the flow boiling correlations indicate that at nucleate boiling dominant region heat transfer rates are increased with increasing heat fluxes, while forced convection effects become prevalent with increasing qualities. Local convective flow boiling heat transfer coefficients and corresponding flow patterns of propane refrigerant were investigated in a 1.0 mm diameter smooth tube by de Oliviera et al. [13]. A high influence of mass and heat fluxes on heat transfer coefficients were observed. Citarella et al. [14] accumulated experimental flow boiling and pressure drop data of R32 and R290 measured in a horizontal smooth stainless-steel tube with a 6.0 mm inner diameter. For a fixed saturation temperature, variational effects of mass flux and heat flux rates were discussed and the compiled experimental data were applied to some of the available reputed flow boiling correlations to assess their predictive performances.

A survey on literature approaches regarding flow boiling of propane reveals that the applicability of the available two-phase flow boiling correlations on this refrigerant still has not been clearly identified. Predictive results obtained by different correlations do not match well with each other's, even considerably disagree most of the time. Therefore, a fair conclusion should be that they cannot be applied for a wide range of working refrigerants over different operational conditions. Further investigation and detailed analysis regarding the estimation capabilities of flow boiling correlations should be provided to make consistent conclusions. One possible reason behind this unclarity and inconsistency between the literature studies is that there are limited experimental data used for correlation development. Furthermore, each experimental study was conducted for its measurements which is one of the main factors that jeopardizing the estimation performance of the proposed correlation as each correlation is developed for a certain range of operating conditions. These operational drawbacks on correlation development procedure can be conquered by developing a novel convective flow boiling correlation founded on R290 data as each refrigerant has an intrinsic thermophysical property. This research study aims to propose an accurate correlation for the saturated flow boiling of propane. From eighteen independent laboratories located in different regions around the world, a database compiled of 2179 experimental data is correlated for developing a new flow boiling model based on R290 data. The proposed flow boiling model provides satisfactory estimations over the compiled experimental database with a mean absolute error value slightly below 20.0%, which is much accurate and reliable than the predictions obtained from most of the flow boiling correlations discussed in this research study.

2 Experimental Database Description for R290

As mentioned in the introduction section, the accumulated data contain 2179 points retrieved from different laboratories around the world as reported in Table 1. Except for one case, all experiments were conducted on stainless steel tubes. Furthermore, horizontal tube orientation is considered for most of the cases. Operational conditions cover for vapor qualities ranging from 0.01 to 0.99, mass fluxes ranging from 50 to 600 kg/m²s, saturation temperatures ranging from − 35.0 to 43.0 °C, imposed heat flux rates ranging from 2.5 to 227.0 kW/m², and hydraulic channel diameters ranging from 0.3 to 7.7 mm. Figure 1 visualizes the distribution of channel diameters and heat flux rates over the experimental database. It is observed that from Fig. 1 that 20.7% of the experimental data fall within the macro-tube range, while 70.1% of the data reside in the mini-tube range, which corresponds to the fact that mini-channel tubes are dominant over the entire database relying on the classification made by Kandlikar [15] that defines a boundary between the conventional and small channels. 56.2% of the heat flux data fall within $q = 0.0–20.0$ kW/m² which implies that low heat flux rates are prevalent over the experimental database. Figure 2a illustrates the distribution of the experimental

points related to vapor qualities and mass velocities for the compiled database. It is seen that 67.4% of the data lie within the region where mass fluxes range between 100 and 300 kg/m²s. Figure 2b shows the data distribution of vapor qualities. The quality band defined in the range of 0.1 and 0.3 accounts for 32.1% of the database. It is also interesting to see that number of experimental vapor quality points decreases with increasing qualities for the compiled database.

Figure 3a visualizes the vapor–liquid phase flow distribution of the database. Considering Re = 2300 as a boundary threshold value between laminar and viscous flow conditions, 38.3% of the data are in the laminar liquid and turbulent vapor range, while 57.4% of the data fall in the turbulent liquid–turbulent vapor region. A very limited ratio of 0.7% of experimental data resides in a laminar liquid–laminar vapor zone, which indicates that turbulence effects dominate the flow condition of the experimental database. Figure 3b shows the distribution of the flow boiling heat transfer coefficients with vapor qualities obtained for R290 experimental data. It is observed that the heat transfer coefficient increases with increasing quality rates until the incipience of the critical heat flux zone then followed by steep declines in heat transfer coefficient values resulted from the dry-out effects until the end of the quality range.

Table 1 Operational conditions of the experimental database for R290

	T_{sat} (°C)	G (kg/m²s)	Q (kW/m²)	x (-)	D_h (mm)	Tube orientation and material	Number of data
Anwar et al. [16]	23.0–43.0	100.0–500.0	60.0–140.0	0.03–0.85	1.7	Vertical stainless-steel tube	40
Chien et al. [17]	10.0	150.0–300.0	10.0–15.0	0.01–0.96	1.5	Horizontal stainless-steel tube	96
Chien et al. [18]	10.0	200.0–350.0	10.0–20.0	0.01–0.80	0.3–1.5	Horizontal stainless-steel tube	141
Choi and Oh [19]	9.0–10.0	120.0–180.0	15.0–25.0	0.01–0.85	3.0	Horizontal stainless-steel tube	65
Citarella et al. [14]	25.0	150.0–300.0	10.0–40.0	0.05–0.98	6.0	Horizontal stainless-steel tube	88
Del col et al. [20]	40.0	100.0–600.0	20.0–105.0	0.05–0.49	0.96	Horizontal stainless-steel tube	27
Allymehr [21]	0.0–10.0	254.0–503.0	15.0–61.0	0.15–0.99	4.2	Horizontal stainless-steel tube	105
Lillo et al. [4]	25.0–35.0	150.0–300.0	2.5–40.0	0.01–0.98	6.0	Horizontal stainless-steel tube	245
Longo et al. [22]	5.0–20.0	100.0–300.0	15.0–30.0	0.11–0.87	4.0	Horizontal stainless-steel tube	62
Maqbool et al. [5]	23.0–43.0	100.0–500.0	40.0–190.0	0.04–0.93	1.7	Vertical stainless-steel tube	115
Maqbool et al. [23]	23.0	100.0–400.0	20.0–227.0	0.02–0.98	1.7	Vertical stainless-steel tube	142
de Oliviera et al. [13]	25.0	240.0–480.0	5.0–60.0	0.01–0.99	1.0	Horizontal stainless-steel tube	358
Pamitran et al. [24]	0.0–10.0	100.0–200.0	10.0–20.0	0.02–0.98	1.5–3.0	Horizontal stainless-steel tube	206
Pamitran et al. [25]	10.0–11.0	50.0–250.0	5.0–30.0	0.01–0.96	1.5–3.0	Horizontal stainless-steel tube	205
Shin et al. [7]	12.0	424.0–583.0	30.0	0.05–0.67	7.7	Horizontal stainless-steel tube	24
Wang et al. [26]	− 35.0– − 14.0	64.0–100.0	11.7–53.1	0.09–0.91	6.0	Horizontal copper tube	41
Wang et al. [27]	− 35.0–− 1.0	70.0–74.0	11.8–53.2	0.10–0.97	6.0	Horizontal stainless-steel tube	55
Zhu et al. [28]	0.0–10.0	200.0–400.0	5.0–15.0	0.08–0.95	2.0	Horizontal stainless-steel tube	67
							2179
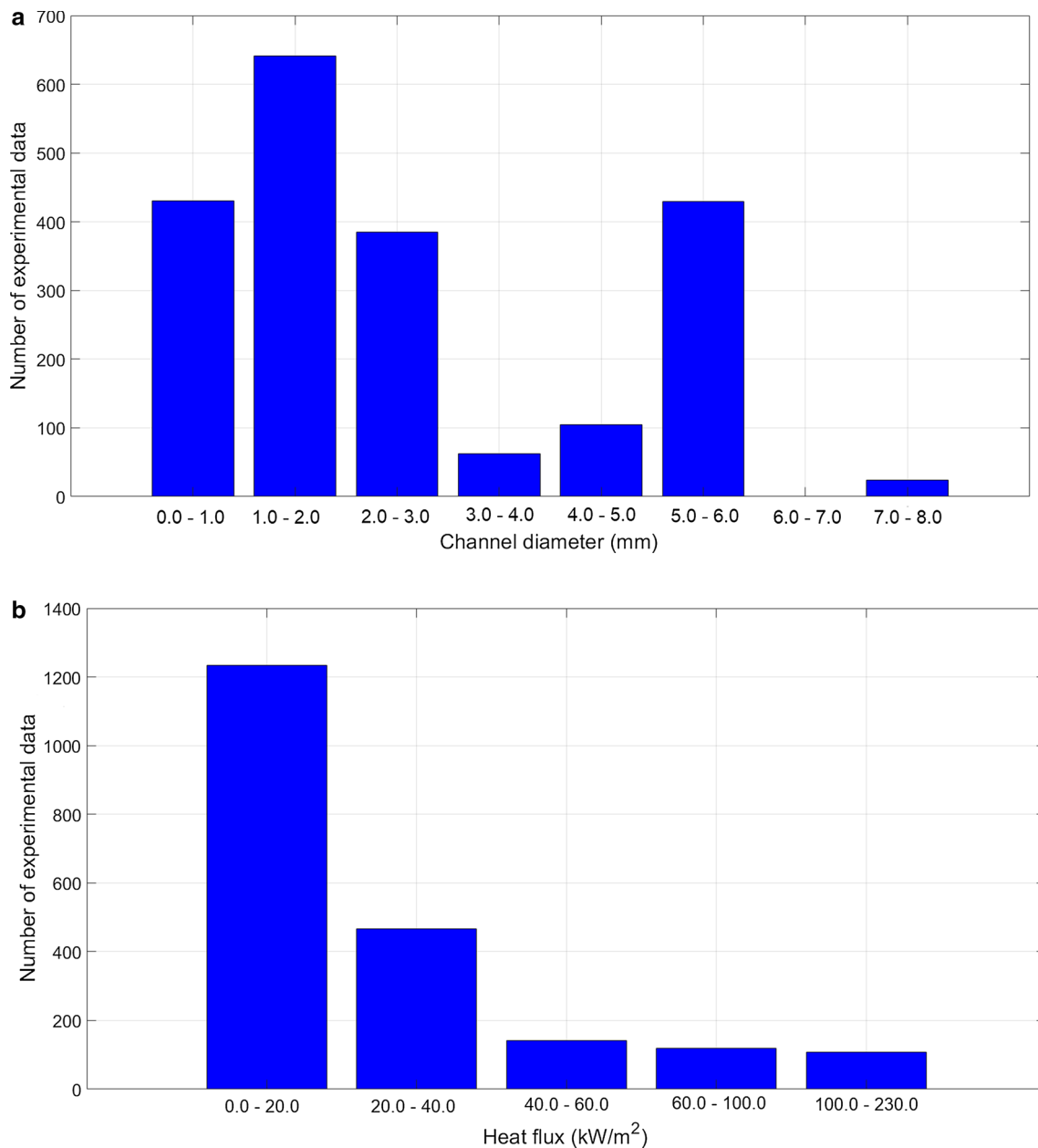
Fig. 1 Distribution of the experimental data for **a** channel diameters and **b** heat fluxes

3 Review of the Literature Correlations Developed for Calculating Saturated Flow Boiling Heat Transfer Coefficients

Three different governing mechanisms dominate the flow boiling heat transfer taken place inside smooth channels. These mechanisms are nucleate boiling, convective boiling, and post-dry-out heat transfer which collectively model the essential heat transfer framework of the two-phase flow boiling process. Post-dry-out heat transfer is characteristically formed by the mist flow stream which is a liquid-deficient flow regime and generally takes place at

higher channel wall temperatures. It is very difficult and tiresome to predict the proclivities and tendencies of the actual heat transfer rates using the developed saturated flow boiling correlations in the corresponding flow boiling regime. A favorable option for predicting the actual heat transfer rates in the post-dry-out flow boiling regime can be to apply the dispersed flow regime heat transfer correlations of Dougal-Rohsenow [29] and Groeneveld [30] which compute the wall heat transfer coefficients as a function of local equilibrium vapor quality and channel wall temperatures. These correlations can predict reasonable trends for this governing flow regime, however,
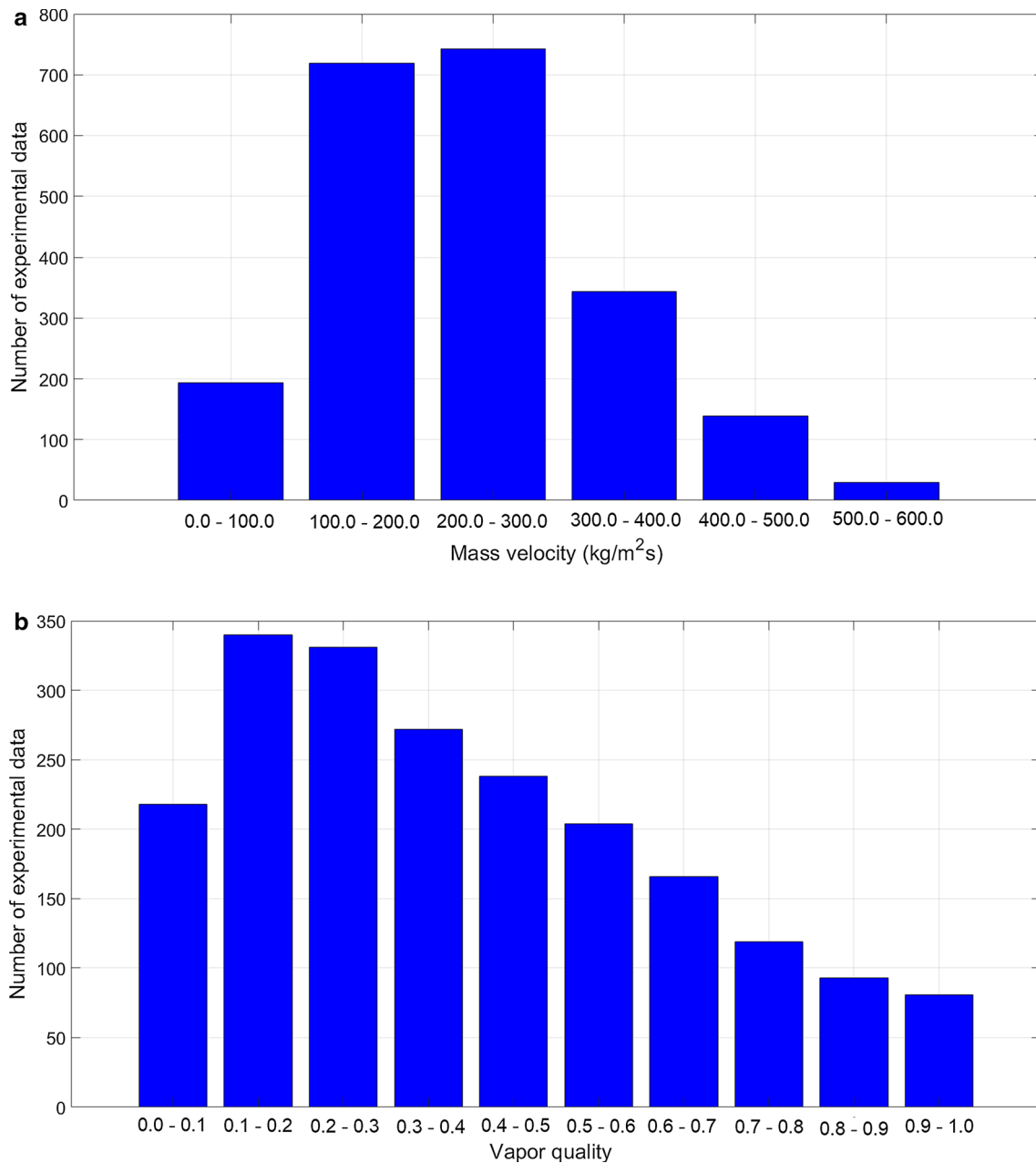
Fig. 2 Distribution of the compiled data points with (**a**) mass velocity and (**b**) vapor quality

sometimes perform unsatisfactory estimations depending on the operational conditions.

Table 2 reports the most frequently used dimensionless numbers in flow boiling models. Two-phase flow boiling correlations are developed by using different combinations of these dimensionless numbers relying on their applicability over different flow boiling mechanisms Flow boiling correlations have been classified into seven categories depending upon the formulation framework of the correlation [2]. These are enhancement-factor, superposition, asymptotic, largest mechanism predominant nucleate boiling, flow pattern-based,

and hybrid type correlations. Post-dry-out effects may not be taken into account in some of the correlation types as they only consider nucleate boiling and/or convective boiling contributions neglecting the effects of mist flow conditions over two-phase flow boiling heat transfer coefficient rates. Flow boiling heat transfer coefficient is represented by the following type of expression in the context of enhancement-factor-type flow boiling models

$$h_{tp} = \tau \cdot h_{sp} \tag{1}$$

a

b
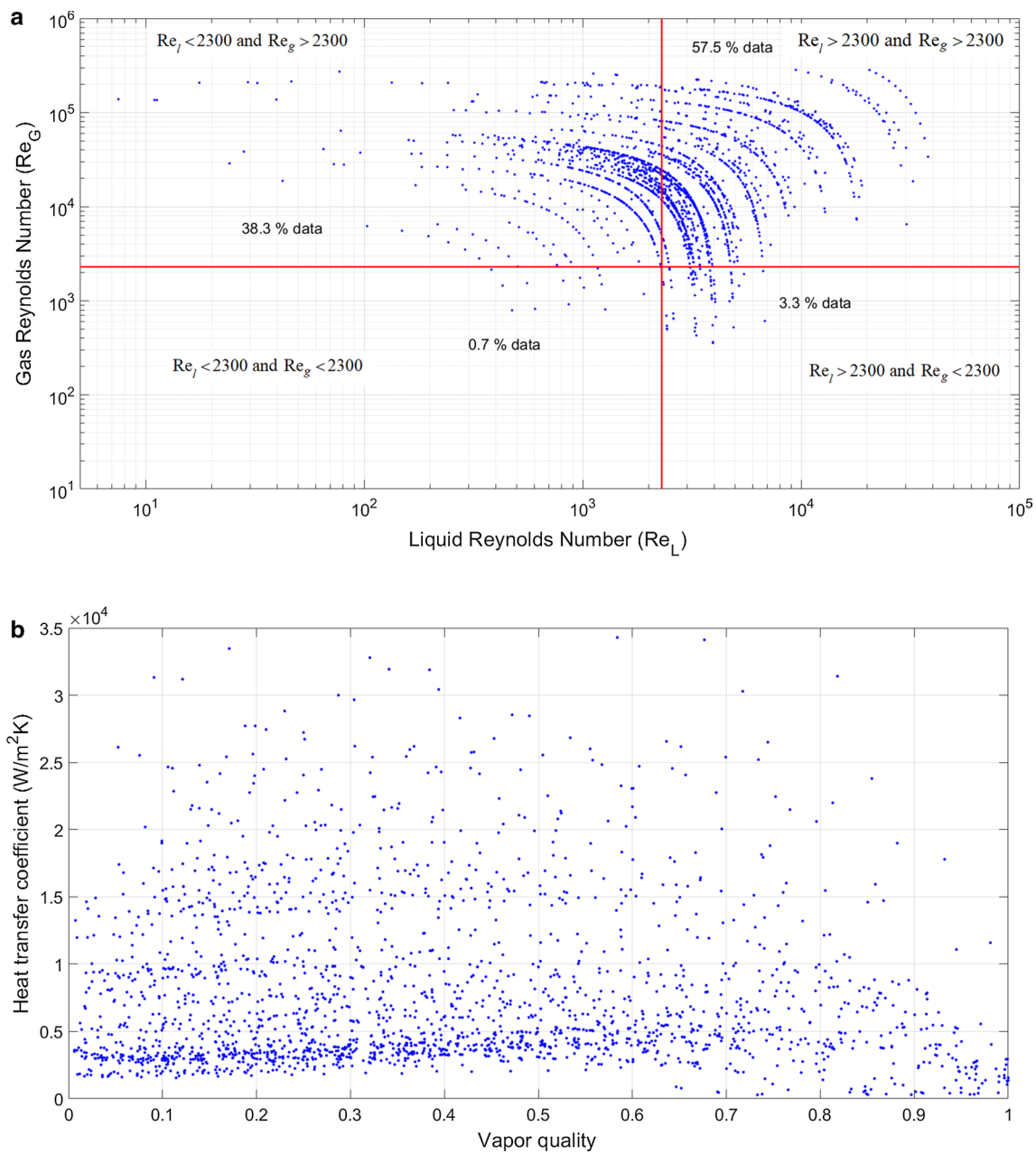
Fig. 3 **a** Laminar-turbulent flow distribution over the entire experimental database. **b** Flow boiling heat transfer coefficient distribution with respect to increasing vapor quality rates

where h_{tp} stands for two-phase heat transfer coefficient, τ is the enhancement factor, and h_{sp} is the single-phase heat transfer coefficient. Between different alternatives for single-phase heat transfer models, Dittus and Boelter [31] correlation is the most frequently used equation whose formulation is given below

$$h_{sp,m} = 0.023 \mathrm{Re}_m^{0.8} \mathrm{Pr}_m^{0.4} \frac{k_m}{D_h} \qquad (2)$$

where m correspondingly represents l for liquid and g for vapor. Among plenty of literature formulations founded on enhancement factor types, correlations of Gungor and Winterton [8], Kenning and Cooper [32], Kew and Cornwell [33], Li and Wu [34], and Yan and Lin [35] are considered for calculating the two-phase heat transfer coefficient of R290 for this research study. Respective formulations and main foundations of these correlations are reported in Table 3.

Table 2 Dimensionless numbers frequently used in the flow boiling models

Dimensionless number	Mathematical definition
Boiling number	$\mathrm{Bo} = \frac{q''}{G \cdot h_{\mathrm{fg}}}$
Liquid Froude number	$\mathrm{Fr_l} = \frac{[G \cdot (1-x)]^2}{(g \cdot D_{\mathrm{h}} \cdot \rho_{\mathrm{l}}^2)}$
Liquid ($m=l$) or vapor ($m=v$) only Froude number	$\mathrm{Fr_{mo}} = \frac{G^2}{g \cdot D_{\mathrm{h}} \cdot \rho_m^2}$
Liquid Reynolds number	$\mathrm{Re_l} = \frac{G \cdot D_{\mathrm{h}} \cdot (1-x)}{\mu_{\mathrm{l}}}$
Vapor Reynolds number	$\mathrm{Re_v} = \frac{G \cdot D_{\mathrm{h}} \cdot x}{\mu_{\mathrm{v}}}$
Liquid ($m=l$) and vapor ($m=v$) only Reynolds number	$\mathrm{Re_{mo}} = \frac{G \cdot D_{\mathrm{h}}}{\mu_m}$
Liquid ($m=l$) and vapor ($m=v$) only Prandtl number	$\mathrm{Pr}_m = \frac{\mu_m \cdot C_{\mathrm{pm}}}{k_m}$
Liquid ($m=l$) and vapor ($m=v$) only Weber number	$\mathrm{We}_m = \frac{G^2 \cdot D_{\mathrm{h}}}{\rho_m \cdot \sigma}$
Bond number	$\mathrm{Bd} = \frac{g \cdot (\rho_{\mathrm{l}} - \rho_{\mathrm{v}}) \cdot D_{\mathrm{h}}}{\sigma}$
Convection number	$\mathrm{Co} = \left(\frac{1-x}{x}\right)^{0.8} \left(\frac{\rho_{\mathrm{v}}}{\rho_{\mathrm{l}}}\right)^{0.5}$
Confinement number	$\mathrm{Conf} = \frac{\sqrt{\left(\frac{\sigma}{g(\rho_{\mathrm{l}} - \rho_{\mathrm{v}})}\right)}}{D_{\mathrm{h}}}$
Lockhart–Martinelli parameter	$X_{\mathrm{tt}} = \left(\frac{1-x}{x}\right)^{0.9} \left(\frac{\rho_{\mathrm{v}}}{\rho_{\mathrm{l}}}\right)^{0.5} \left(\frac{\mu_{\mathrm{l}}}{\mu_{\mathrm{v}}}\right)^{0.1}$

Table 3 Formulations of some of the enhancement-type flow boiling correlations

Correlation	Formulation	Comments
Gungor and Winterton [8]	$h_{\mathrm{tp}} = \left(S \cdot S_2 + F \cdot F_2\right) h_{\mathrm{cb,l}}$ where $h_{\mathrm{cb,l}}$ can be calculated by Dittus and Boelter [31] correlation given in Eq. 2 $S = 1 + 3000\mathrm{Bo}^{0.86}$ $F = 1.12\left(\frac{x}{1-x}\right)^{0.75}\left(\frac{\rho_{\mathrm{l}}}{\rho_{\mathrm{v}}}\right)^{0.41}$ $S_2 = \begin{cases} \mathrm{Fr_{lo}^{1/2}} & \text{if horizontal and } \mathrm{Fr_{lo}} < 0.05 \\ 1 & \text{otherwise} \end{cases}$ $F_2 = \begin{cases} \mathrm{Fr_{lo}^{(0.1-2.0Fr_{lo})}} & \text{if horizontal and } \mathrm{Fr_{lo}} < 0.05 \\ 1 & \text{otherwise} \end{cases}$	Based on the compiled 3693 data points from R11, R12, R22, R113, R114, and R718 refrigerants
Kenning and Cooper [32]	$h_{\mathrm{tp}} = \left(1 + 1.8X_{\mathrm{tt}}^{-0.87}\right) h_{\mathrm{cb,l}}$ where $h_{\mathrm{cb,l}}$ is computed by Dittus and Boelter [31] correlation formulated in Eq. 2 and liquid turbulent/gas turbulent Martinelli parameter X_{tt}	
Kew and Cornwell [33]	$h_{\mathrm{tp}} = 30\mathrm{Re_{lo}^{0.857}}\mathrm{Bo}^{0.714}\left(\frac{1}{1-x}\right)^{0.143}\frac{k_{\mathrm{l}}}{D_{\mathrm{h}}}$	Built on R141b refrigerant database compiled of 697 data points
Li and Wu [34]	$h_{\mathrm{tp}} = 334\mathrm{Bo}^{0.3}\left(\mathrm{Bd} \cdot \mathrm{Re_l^{0.36}}\right)^{0.4}\frac{k_{\mathrm{l}}}{D_{\mathrm{h}}}$	Based on the compiled database of eight different refrigerants comprised of 3744 points
Yan and Lin [35]	$h_{\mathrm{tp}} = \left(C_1 \cdot Co^{C_2} + C_3 \cdot \mathrm{Bo}^{C_4} \cdot \mathrm{Fr_{lo}}\right)(1-x)\frac{4.364 \cdot k_{\mathrm{l}}}{D_{\mathrm{h}}}$ where correlation constants of C_1, C_2, C_3, C_4 are direct functions of liquid only Reynolds number ($\mathrm{Re_{lo}}$) and reduced temperature ($T_{\mathrm{R}} = T_{\mathrm{sat}}/T_{\mathrm{crit}}$)	Based on R134a experimental data obtained in 2.0 mm ID smooth tubes

Table 4 Respective formulations of superposition type flow boiling models

Correlation	Formulation	Comments
Gungor and Winterton [37]	$h_{tp} = S \cdot S_2 \cdot h_{nb} + F \cdot F_2 \cdot h_{cb}$ where h_{nb} is calculated by Cooper [41] correlation in Table 5, while h_{cb} is computed by Dittus and Boelter [31] equation formulated in Eq. 2 $S_2 = \begin{cases} Fr_{lo}^{1/2} & \text{if horizontal and } Fr_{lo} < 0.05 \\ \text{otherwise} \end{cases}$ $F_2 = \begin{cases} Fr_{lo}^{(0.1-2.0Fr_{lo})} & \text{if horizontal and } Fr_{lo} < 0.05 \\ \text{otherwise} \end{cases}$ $S = 1/\left(1 + 1.15 \times 10^{-6} F^2 Re_l^{1.17}\right)$ $F = 1 + 2.4 \times 10^4 Bo^{.16} + 1.37 X_{tt}^{-0.86}$ where turbulent liquid/turbulent vapor Lockhart–Martinelli parameter given in Table 2	The database compiled from 4300 experimental points of R11, R12, R22, R113, R114, R718, and ethylene glycol
Jung et al. [38]	$h_{tp} = \left(\frac{S}{M_1}\right) \cdot h_{nb} + M_2 \cdot F \cdot h_{cb}$ h_{cb} is calculated by liquid only Dittus and Boelter [31] equation given in Eq. 2, whereas h_{nb} is calculated by Stephan and Abdelselam [42] nucleate pool boiling correlation given below $h_{nb} = 207 \left(\frac{k_l}{md}\right) \left(\frac{q \cdot md}{k_l \cdot T_{sat}}\right)^{0.745} \left(\frac{\rho_v}{\rho_l}\right)^{0.581} Pr_l^{0.533}$ $md = 0.0146\beta \left(\frac{2\sigma}{g(\rho_l - \rho_v)}\right)^{0.5}$ where contact angle is considered to be $\beta = 35^o$ $S = \begin{cases} 4048 X_{tt}^{1.22} Bo^{1.13} & \text{if } X_{tt} < 1 \\ 2.0 - 0.1 X_{tt}^{-0.28} Bo^{-0.33} & \text{if } 1 \leq X_{tt} \leq 5 \end{cases}$ $F = 2.37 \left(0.29 + \left(\frac{1}{X_{tt}}\right)\right)^{0.85}$ where M_1 and M_2 are correlation constants which are equal to 1.0 for pure fluids, and X_{tt} is the turbulent liquid/turbulent vapor Martinelli parameter	Correlated for 1588 experimental data of pure refrigerants R22, R114, R12, R152a and R500 and 1268 data points of R22/ R114 and R12/R152 refrigerant mixtures
Choi et al. [39]	$h_{tp} = S \cdot h_{nb} + F \cdot h_{cb}$ where h_{nb} is calculated by Cooper [41] correlation formulated in Table 5 and h_{cb} is computed by Eq. 2 $S = 7.2694 \left(\phi_l^2\right)^{0.0094} Bo^{0.2814}$ $F = 0.05 \left(\phi_l^2\right) + 0.95$ where the term ϕ_l^2 is given by the following formulation $\phi_l^2 = 1 + \frac{C}{X_{tt}} + \frac{1}{X_{tt}^2}$ With Lockhart–Martinelli parameter X_{tt} computed by $X_{tt} = \left(\frac{1-x}{x}\right)^{7/8} \left(\frac{\mu_l}{\mu_v}\right)^{1/8} \left(\frac{\rho_v}{\rho_l}\right)^{1/2}$ And Chisholm parameter C is calculated by the below-given procedure $C = \begin{cases} 10 & \text{if } (Re_l > 2000) \text{ and } (Re_v < 1000) \\ 20 & \text{if } (Re_l > 2000) \text{ and } (Re_v > 2000) \\ 5 & \text{if } (Re_l < 1000) \text{ and } (Re_v < 1000) \\ 12 & \text{if } (Re_l < 1000) \text{ and } (Re_v > 2000) \end{cases}$	Based on experimental data of CO_2

Correlation	Formulation	Comments
Mahmoud and Karayiannis [40]	$h_{tp} = S \cdot h_{nb} + F \cdot h_{cb}$ where h_{nb} is obtained by Cooper [41] correlation $h_{cb} = \begin{cases} 4.36 \dfrac{k_l}{D_h} & \text{Re}_l < 2000 \\[2mm] 0.023 \text{Re}_l^{0.8} \text{Pr}_l^{0.4} \dfrac{k_l}{D_h} & \text{Re}_l > 3000 \end{cases}$ $F = \left(1 + \frac{2.812 \cdot \text{Conf}^{-0.408}}{X_{tt}}\right)$ where Lockhart–Martinelli X_{tt} parameter is computed by $X_{tt} = \left(\frac{1-x}{x}\right)\left(\frac{f_l}{f_v}\right)^{0.5}\left(\frac{\rho_v}{\rho_l}\right)^{0.5}$ $S = \left[1 + 2.56 \times 10^{-6}\left(\text{Re}_l F^{1.25}\right)^{1.17}\right]^{-1}$	Correlated for 5152 experimental data points of R134a obtained in smooth tubes with D = 0.52, 1.1, 2.01, 2.88, and 4.26 ID

Chen [36] pioneered the evolution of superposition type flow boiling models with his groundbreaking two heat transfer correlation; thereafter, these types of developed correlations are also called Chen-type models. Chen [36] conceptualized that the two-phase flow boiling process is under the effect of two complementary mechanisms of nucleate boiling and convective boiling, which is mathematically modeled by the following expression

$$h_{tp} = S \cdot h_{nb} + F \cdot h_{sp} \tag{3}$$

where h_{nb} symbolizes the nucleate flow boiling heat transfer coefficient; h_{sp} is the single-phase heat transfer coefficient; S is the suppression factor responsible for suppressing the nucleate boiling effects in the two-phase flow; and convective boiling correction factor F describes the enhancement in convection effects in two-phase flows. Post-dry-out effects have been excluded in Chen-type correlations. Well-reputed correlations of Gungor–Winterton [37], Jung et al. [38], Choi et al. [39], and Mahmoud and Karayiannis [40] have

been considered as favorable members of superposition type models whose formulations are reported in Table 4.

Heat transfer coefficients of the nucleate boiling models do not vary as a function of vapor qualities and only consider the influences of nucleate boiling sites neglecting the effects of convective boiling contributions. Well-known nucleate boiling correlations of Cooper [41], Sun and Mishima [43], Lazarek and Black [44], Hamdar et al. [45], Tran et al. [46], and Yu et al. [47] are given in Table 5.

Asymptotic flow boiling models take into account the contributions of convective boiling and nucleate boiling in the below-given form of formulation

$$h_{tp} = \left[\left(S \cdot h_{nb}\right)^k + \left(F \cdot h_{cb}\right)^k\right]^{1/k} \tag{4}$$

Table 6 provides some of the prominent asymptotic flow boiling models of Liu—Winterton [48] and Wattelet et al. [49].

Table 5 Review of nucleate boiling-based two-phase heat transfer correlations

Correlation	Formulation	Comments
Cooper [41]	$h_{nb} = 55 p_r^{0.12-0.087\ln(\varepsilon)}\left(-0.4343\ln(p_r)\right)^{-0.55} M^{-0.5} q^{0.67}$ where ε is the surface roughness in μm	Based on nearly 6000 experimental nucleate boiling data
Sun and Mishima [43]	$h_{nb} = \dfrac{6.0 \text{Re}_{lo}^{1.05} \text{Bo}^{0.54}}{\text{We}_{lo}^{0.191}\left(\frac{\rho_l}{\rho_v}\right)^{0.142}}$	Based on 2505 experimental data points of 11 different refrigerants
Lazarek and Black [44]	$h_{nb} = 30 \text{Re}_{lo}^{0.857} \text{Bo}^{0.714} \dfrac{k_l}{D_h}$	Based on 738 data points of R113 refrigerant
Hamdar et al. [45]	$h_{nb} = 6942.8\left(\text{Bo}^2\text{We}_{lo}\right)^{0.2415}\left(\rho_v/\rho_l\right)^{0.22652}\left(k_l/D_h\right)$	Based on R152 experimental data
Tran et al. [46]	$h_{nb} = 840,000 \text{Bo}^{0.6}\text{We}_{lo}^{0.3}\left(\frac{\rho_l}{\rho_v}\right)^{-0.4}$	Based on R12 experimental data
Yu et al. [47]	$h_{nb} = 640,000 \text{Bo}^{0.54}\text{We}_{lo}^{0.27}\left(\frac{\rho_l}{\rho_v}\right)^{-0.2}$	Based on R134 experimental data

The largest mechanism predominant models compute the heat transfer coefficients obtained from different governing mechanisms and retain the highest calculated coefficient between them. Most of the literature flow boiling correlations constructed in the context of the largest mechanism predominant model consider the nucleate and convective boiling effects as dominant mechanisms. Correlations of Shah [50], Kandlikar [51] and Ducoulombier et al. [52] are the most applied flow boiling models belonging to this category. Table 7 reports the corresponding formulations and valid ranges of these mentioned correlations.

Hybrid flow boiling models are excluded from this research study because of their incapability in estimating the two-phase flow boiling heat transfer of propane. Flow pattern-based models necessitate the flow pattern information of the related refrigerant to calculate the two-phase flow boiling heat transfer coefficient, which complicates their successful implementation over a wide range of refrigerant types. Therefore, flow boiling models falling into this category are also not considered for this research study due to the unavailable flow pattern information for the R290 refrigerant.

4 Comparison of the Predictive Performances of the Existing Correlations for Propane Experimental Data

Prediction accuracies of the existing two-phase flow boiling models discussed in the previous section are evaluated based on the database compiled of 2179 experimental points of propane. Two different performance indexes are considered including mean absolute error (MAE) and mean relative error (MRE) for performance assessment of the compared correlations. MAE is used to assess the overall estimation accuracy, whereas MRE is applied to gauge whether overprediction or underprediction is occurred by the employed correlation over the related database.

$$\text{MAE} = \frac{1}{N} \sum_{i=1}^{N} \left| \frac{h_{\text{calc}}^i - h_{\text{exp}}^i}{h_{\text{exp}}^i} \right| \tag{5}$$

$$\text{MRE} = \frac{1}{N} \sum_{i=1}^{N} \frac{h_{\text{calc}}^i - h_{\text{exp}}^i}{h_{\text{exp}}^i} \tag{6}$$

where N is the total number of the experimental data in the compiled database. Thermophysical properties of propane refrigerant are obtained using the REFPROP package from the NIST laboratory [53].

Table 8 lists the error analysis of the compared correlations over the entire experimental database. It is observed that correlations of Cooper [41] (28.6%), Liu–Winterton [48] (29.6%), and Sun–Mishima [43] (29.9%) obtain

Table 6 Formulations of the asymptotic flow boiling correlations employed in this research study

Correlation	Formulation	Comments
Liu and Winterton [48]	$h_{\text{tp}} = \left[\left(S \cdot h_{\text{nb}} \right)^2 + \left(F \cdot h_{\text{cb}} \right)^2 \right]^{0.5}$ where h_{nb} is calculated by Cooper [41] correlation and h_{cb} is computed by Dittus–Boelter [31] formulation $S = \left(1 + 0.055 F^{0.1} \text{Re}_l^{0.16} \right)^{-1}$ $F = \left(1 + x \cdot \text{Pr}_l \left(\frac{\rho_l}{\rho_v} - 1 \right) \right)^{0.35}$	Based on 4183 data points of water, R12, R22, R11, R113, R114, ethylene glycol, n-butanol, ethanol
Wattelet et al. [49]	$h_{\text{tp}} = \left[h_{\text{nb}}^{2.5} + \left(F \cdot R \cdot h_{\text{cb}} \right)^{2.5} \right]^{1/2.5}$ where h_{nb} is calculated by Cooper [41] correlation and h_{cb} is computed by Dittus–Boelter [31] formulation $R = \begin{cases} 1.32 \text{Fr}_{\text{lo}}^{0.2} & \text{if Fr}_{\text{lo}} < 0.25 \\ 1 & \text{if Fr}_{\text{lo}} > 0.25 \end{cases}$ $F = 1 + 1.925 \cdot X_{\text{tt}}^{-0.83}$	Verified for their own measurement of experimental data for R12, R134a and mixture flowing in a 7.04-mm ID smooth tube

Table 7 Some of the well-reputed largest mechanism dominant flow boiling models

Correlation	Formulation	Comments
Shah [50]	Largest between the below-defined correlations is the ultimate h_{tp} $h_{tp} = 230Bo^{0.5}h_{cb}$ $h_{tp} = 1.8\left(Co\left(0.38Fr_{lo}^{-0.3}\right)^n\right)^{-0.8}h_{cb}$ $h_{tp} = F \cdot \exp\left(2.47\left(Co\left(0.38Fr_{lo}^{-0.3}\right)^n\right)^{-0.15}\right)h_{cb}$ $h_{tp} = F \cdot \exp\left(2.74\left(Co\left(0.38Fr_{lo}^{-0.3}\right)^n\right)^{-0.1}\right)h_{cb}$ where h_{cb} is calculated by Dittus–Boelter [32] equation $F = \begin{cases} 14.7Bo^{0.5} & \text{if } Bo \geq 0.0011 \\ 15.4Bo^{0.5} & \text{if } Bo < 0.0011 \end{cases}$ $n = \begin{cases} 0 & \text{if vertical tube or horizontal tube with } Fr_{lo} \geq 0.04 \\ 1 & \text{if horizontal tube with } Fr_{lo} < 0.04 \end{cases}$	The database compiled of 760 data points from 19 different sources covering refrigerants of R11, R12, R22, R113, and cyclohexane
Kandlikar [51]	$h_{tp} = \max\left(h_{nb}, h_{cb}\right)$ $h_{nb} = \left(0.6683Co^{-0.2}f\left(Fr_{lo}\right) + 1058.0Bo^{0.7}F_f\right)h_l$ $h_{cb} = \left(1.136Co^{-0.9}f\left(Fr_{lo}\right) + 667.2Bo^{0.7}F_f\right)h_l$ $f\left(Fr_{lo}\right) = \begin{cases} \left(25Fr_{lo}\right)^{0.3} & \text{for horizontal tubes with } Fr_{lo} \leq 0.04 \\ 1 & \text{otherwise} \end{cases}$ where h_l is calculated by Eq. 2. The fluid-specific parameter is $F_f = 1$ when stainless-steel tubes are used. The numerical value of F_f is tabulated in the below table for copper and brass tubes {table below}	Validated against 5246 data points obtained from 24 different experimental sources Valid for operational condition range given: $D_h = 4.6$–32.0 mm, $G = 13$–8179 kg/m²s, $x = 0.001$–0.987
Ducoulombier et al. [52]	$h_{tp} = \max\left(h_{nb}, h_{cb}\right)$ $h_{nb} = 131p_r^{-0.0063}\left(-0.4343\ln\left(p_r\right)\right)^{-0.55}M^{-0.5}q^{0.58}$ $h_{cb} = \begin{cases} \left[1.47 \times 10^4 Bo + 0.93\left(X_{tt}\right)^{-2/3}\right]h_l & \text{if }\left(Bo > 1.1 \times 10^{-4}\right) \\ \left[1 + 1.8\left(X_{tt}\right)^{-0.986}\right]h_l & \text{if }\left(Bo < 1.1 \times 10^{-4}\right) \end{cases}$ where h_l is computed by Eq. 2 and X_{tt} is turbulent liquid/turbulent vapor Lockhart–Martinelli parameter	Experimental data of CO_2 based on their own measurements. Operational conditions cover $T_{sat} = -10.0, -5.0, 0.0$ °C $G = 200.0$–1200.0 kg/m²s $Q = 10, 20, 30$ kW/m² $D = 0.529$ mm

Refrigerant	F_f	Refrigerant	F_f
R114	1.24	R124	1.00
R113	1.30	R141b	1.80
R22	2.20	R32/R132	3.30
R131B	1.31	R134a	1.63
R12	1.50	R152a	1.10
R11	1.30	Nitrogen	4.70
R718	1.00	Neon	3.50

the lowest deviations rates, which are the top three best performing correlations between the compared methods. These correlations, respectively, have a MRE of 1.7%, 2.0%, and −11.3%, which explains that there is an evident underprediction that occurred by the Sun-Mishima [43] correlation, while negligible overprediction is performed by the remaining two correlations. It is also interesting to see that two out of three top correlations (Cooper [41] and Sun-Mishima [43]) whose MAE is below 30.0% are nucleate boiling type models, verifying that the overall experimental database is dominated by data points under the effect of nucleate boiling sites. Flow boiling models proposed by Wattelet et al. [49], Ducoulumbier et al. [52], Kew-Cornwell [33], Choi et al. [39], and Gungor—Winterton [8] have, respectively, MAE of 30.3%, 31.1%, 35.9, 36.9%, and 39.5%. Between them, underprediction over the entire experimental database is evident for Choi et al. [41] correlation, with a MRE of -28.0%. Remaining flow boiling correlations given in Table 8 which are Lazarek—Black [44], Gungor—Winterton [37], Jung et al. [38], Shah [50], Kandlikar [51], and Hamdar et al. [45] in the error zone with corresponding MAE values of 40.3%, 42.2%, 43.1%, 45.5%, 47.1%, and 100.2%. A nucleate boiling type flow boiling correlation developed by Hamdar et al.

Table 8 Estimation performance of the literature flow boiling correlations for propane

Flow boiling correlation	MAE (%)	MRE (%)	ξ_{20} (%)	ξ_{30} (%)	ξ_{40} (%)
Cooper [41]	28.6	1.7	50.0	65.1	77.2
Liu and Winterton [48]	29.6	2.0	43.8	62.2	74.3
Sun and Mishima [43]	29.9	− 11.3	37.5	53.2	71.9
Wattelet et al. [49]	30.3	− 20.1	33.5	55.0	75.3
Ducoulumbier et al. [52]	31.1	− 20.8	31.3	52.7	72.8
Kew and Cornwell [33]	35.9	14.8	50.0	64.2	70.0
Choi et al. [39]	36.9	− 28.0	21.3	38.7	62.0
Gungor and Winterton [8]	39.5	8.6	37.3	51.7	64.5
Lazarek and Black [44]	40.3	24.8	49.3	60.1	68.0
Gungor and Winterton [37]	42.2	− 26.8	19.5	32.7	46.2
Jung et al. [38]	43.1	− 28.8	26.9	42.0	51.5
Shah [50]	45.5	20.5	35.2	46.9	59.0
Kandlikar [51]	47.1	24.1	36.6	48.5	59.6
Hamdar et al. [45]	100.2	66.8	34.8	45.2	57.4

[47] considerably fails to estimate the correct trends of the heat transfer coefficients of the experimental database and greatly overestimates the experimental data with a MRE of 66.8%, which is much higher than those acquired by the flow boiling models compared in Table 8. Percentage of the experimental data estimated within ± 30.0% and ± 40.0% error zones is, respectively, 65.1% and 77.2% for Cooper [41] correlation. Then, followed by Liu – Winterton [48] correlation with a percentage of experimental data predicted within ± 30.0% and ± 40.0% error bands

are correspondingly 62.2% and 74.3%. Tables 9 and 10 demonstrate the predictive performances of each compared correlation for different experimental databases. Most of the compared correlations fail to accurately estimate the experimental databases obtained from Chien et al. [17], Citarella et al. [14], Allymehr [21], and Lillo et al. [4].

Figures 4, 5 and 6 show error band representations of the experimental vs. estimated data along with the prediction accuracies of the two-phase flow boiling heat transfer coefficients for increasing vapor qualities. Overprediction

Table 9 Deviation results of the compared correlations for different experimental databases

Database	Cooper [41]		Wattelet et al. [49]		Liu and Winterton [48]		Ducoulombier et al. [52]		Sun and Mishima [43]		Kew and Cornwell [33]		Lazarek and Black [44]	
	MAE	MRE	MAE	MRE	MAE	MRE	MAE	MRE	MAE	MRE	MAE	MRE	MAE	MRE
Anwar et al. [16]	8.1	− 6.3	8.3	− 7.5	14.1	11.8	13.6	− 13.2	7.1	− 3.6	9.7	0.1	11.5	7.1
Chien et al. [17]	17.2	− 14.5	45.8	− 45.8	30.7	− 30.3	37.9	− 37.8	38.2	− 38.2	15.3	− 10.3	15.1	− 4.1
Chien et al. [18]	59.3	39.4	48.3	− 9.5	57.6	17.4	50.4	2.1	55.2	6.7	68.2	51.5	73.5	60.3
Choi and Oh [19]	23.8	− 20.6	31.6	− 31.6	19.6	− 13.4	37.1	− 37.1	28.5	− 28.1	17.1	− 7.2	17.7	1.4
Citarella et al. [14]	39.7	27.2	25.9	11.1	57.2	46.9	21.7	7.3	39.3	27.3	76.2	63.7	92.3	84.1
Del col et al. [20]	19.1	17.1	17.1	14.6	35.5	35.4	9.6	4.1	8.4	3.5	25.3	25.3	28.7	28.7
Allymehr [21]	50.1	− 50.1	66.1	− 66.1	46.9	− 46.9	58.8	− 58.8	55.2	− 55.2	52.9	− 52.9	42.6	− 42.4
Lillo et al. [4]	53.9	42.1	28.5	13.1	62.2	52.2	26.3	9.1	49.3	38.1	97.6	86.2	115.1	107.7
Longo et al. [22]	14.6	14.1	4.5	− 3.7	25.5	25.5	9.3	− 6.7	8.1	7.1	34.2	34.2	49.2	49.2
Maqbool et al. [5]	10.7	8.9	12.1	− 10.4	10.1	8.6	17.5	− 15.7	11.7	− 6.8	12.7	− 6.9	10.3	− 0.1
Maqbool et al. [23]	11.9	− 11.6	13.4	− 13.3	6.8	3.9	21.8	− 21.8	13.9	− 13.4	12.7	− 8.3	10.8	− 3.3
de Oliviera et al. [13]	26.5	12.3	25.9	− 20.6	18.4	− 3.9	23.9	− 16.4	22.2	− 18.5	27.5	11.4	28.6	17.4
Pamitran et al. [24]	23.2	− 19.1	33.5	− 33.5	23.1	− 15.1	37.3	− 37.3	29.7	− 29.2	17.3	− 5.8	22.1	2.5
Pamitran et al. [25]	19.1	− 14.4	35.2	− 35.2	24.5	− 20.8	36.6	− 36.6	31.5	− 31.2	21.5	2.7	23.5	9.1
Shin et al. [7]	17.8	− 11.1	31.1	− 31.1	18.4	8.6	25.1	− 25.1	19.0	− 15.2	15.1	1.8	20.1	9.2
Wang et al. [26]	13.5	− 13.5	22.5	− 22.5	5.0	− 2.8	37.9	− 37.9	5.3	− 3.4	5.8	0.1	12.3	12.3
Wang et al. [27]	19.4	− 15.2	25.8	− 25.8	9.8	− 5.1	37.9	− 37.9	10.8	− 6.5	10.8	2.1	16.3	16.2
Zhu et al. [28]	25.6	− 1.1	50.6	− 50.6	28.4	− 18.5	43.4	− 43.4	29.0	− 27.2	24.8	1.6	34.1	14.9

Table 10 Prediction accuracies of the compared correlations for various databases

Database	Gungor and Winteron [8]		Choi et al. [39]		Kandlikar [51]		Shah [50]		Hamdar et al. [45]		Jung et al. [38]		Gungor and Winterton [37]	
	MAE	MRE	MAE	MRE	MAE	MRE	MAE	MRE	MAE	MRE	MAE	MRE	MAE	MRE
Anwar et al. [16]	43.2	43.0	27.1	− 27.1	72.6	72.6	67.9	67.9	12.6	10.7	67.9	67.9	12.1	− 9.2
Chien et al. [17]	40.4	− 40.3	45.6	− 45.6	34.1	− 33.5	36.3	− 35.7	42.1	− 42.1	36.3	− 35.7	59.9	− 59.9
Chien et al. [18]	63.1	11.0	54.7	− 2.7	69.3	26.2	69.1	23.1	697.1	614.9	69.1	23.1	73.7	− 8.3
Choi and Oh [19]	15.7	− 9.0	41.1	41.1	12.3	0.1	13.7	− 0.1	16.3	− 0.1	13.7	− 0.1	45.4	− 45.4
Citarella et al. [14]	85.7	78.9	26.7	− 2.3	106.1	99.9	102.1	95.9	192.1	188.1	102.1	95.9	33.5	23.5
Del col et al. [20]	42.6	42.6	11.8	6.8	55.1	55.1	64.9	64.9	17.8	− 17.2	64.9	64.9	17.1	− 17.1
Allymehr [21]	53.2	− 53.2	75.9	− 75.9	53.1	− 48.8	53.1	− 53.1	18.3	− 11.8	53.1	− 53.1	63.1	− 63.1
Lillo et al. [4]	90.3	84.9	29.1	3.4	115.1	110.5	108.4	102.5	217.5	214.3	108.4	102.5	40.7	30.7
Longo et al. [22]	37.3	37.3	18.8	− 18.5	53.6	53.5	50.0	49.6	85.5	85.5	50.0	49.6	12.6	− 10.9
Maqbool et al. [5]	35.6	35.5	29.3	− 29.3	64.8	64.8	59.2	59.2	12.7	10.7	59.2	59.2	17.1	− 9.7
Maqbool et al. [23]	21.7	20.4	29.2	− 29.2	42.7	43.4	39.8	39.8	8.7	0.1	39.8	39.8	22.9	− 22.6
de Oliviera et al. [13]	19.7	− 11.1	26.8	− 23.1	19.7	5.1	19.8	1.3	34.9	− 34.7	19.8	1.3	42.4	− 42.4
Pamitran et al. [24]	20.9	− 15.1	41.5	− 41.5	17.1	− 7.1	17.6	− 7.8	23.5	− 5.8	17.6	− 7.8	48.5	− 48.5
Pamitran et al. [25]	25.0	− 21.3	37.2	− 37.2	19.9	− 11.1	21.4	− 12.3	26.4	− 17.3	21.4	− 12.3	51.7	− 51.7
Shin et al. [7]	14.9	− 13.6	34.1	− 34.1	5.6	3.2	5.6	− 5.1	153.8	153.8	5.6	− 5.1	22.8	− 22.8
Wang et al. [26]	13.4	7.6	48.3	− 48.3	22.4	20.8	14.7	10.5	79.7	79.7	14.7	10.5	28.5	− 28.1
Wang et al. [27]	20.5	15.1	49.2	− 49.2	34.3	29.7	25.4	20.4	74.9	74.9	25.4	20.4	27.3	− 26.5
Zhu et al. [28]	41.5	− 41.5	53.9	− 53.9	37.8	− 37.6	41.5	− 41.5	25.1	− 19.7	41.5	− 41.5	57.9	− 57.9

of the actual data is significantly observed at lower qualities for each correlation in the figures, whereas at higher qualities, particularly between 0.8 and 1.0, the top six best performing correlations considerably underestimate the experimental data due to the influences of the post-dry-out (mist flow) region, in which corresponding heat transfer coefficients drastically decrease. These correlations are not able to trace these sharp variational changes in heat transfer coefficients with regard to increasing vapor qualities; therefore, discrepancies occur between the actual and calculated heat transfer coefficient rates in different regions of the vapor quality span. Comprehensive analysis over estimation capabilities of the existing correlations indicates that there is a need for a new correlation that can accurately predict the two-phase flow boiling heat transfer coefficient of propane refrigerant. The next section deals with the development procedure for the saturated flow boiling correlation based on the propane experimental data.

5 Correlation Development Procedure for R290

Exhaustive numerical tests have been conducted as to which correlation performs best for predicting the saturated flow boiling heat transfer coefficients of propane refrigerant. Based on 2179 data points retained from different sources around the world, a flow boiling correlation constructed by the modified version of Wattelet et al. [51] flow boiling model is proposed. Flow boiling

heat transfer data given in the graphics and charts for the respective source are digitized by a developed Java program to process the available information for developing a novel flow boiling model. Fang et al. [54] proposed to utilize the dimensionless numbers and operational parameters from the literature correlations providing better predictive performances in their novel flow boiling model founded on water flow boiling experimental data. This study adopts similar correlation development procedure, benefiting from the dimensionless numbers of the top two best performing correlations of Cooper [41] and Liu–Winterton [48]. While examining the available correlations thoroughly, it is comprehended that Wattelet et al. [49] correlation covers all beneficial dimensionless numbers along with physical parameters that enable these two correlations to yield minimum deviation results. Based on the flow boiling model of the Wattelet et al. [49], the proposed saturated two-phase flow boiling model framework can be generalized into the below given final form of

$$X_{tt} = \left(\frac{1-x}{x}\right)^{C_1} \cdot \left(\frac{\rho_v}{\rho_l}\right)^{C_2} \cdot \left(\frac{\mu_l}{\mu_v}\right)^{C_3}$$

$$F = 1 + C_4 \cdot X_{tt}^{C_5}$$

$$h_{nb} = C_6 \cdot p_r^{C_7} \cdot \left(-\log\left(p_r\right)\right)^{C_8} \cdot M^{C_9} \cdot Q^{C_{10}}$$

$$h_{cb} = C_{11} \cdot Re_l^{C_{12}} \cdot Pr_l^{C_{13}} \cdot \left(k_l/D_h\right)$$ (7)

$$h_{tp} = \left(h_{nb}^{C_{14}} + \left(F \cdot h_{cb}\right)^{C_{14}}\right)^{1/C_{14}}$$
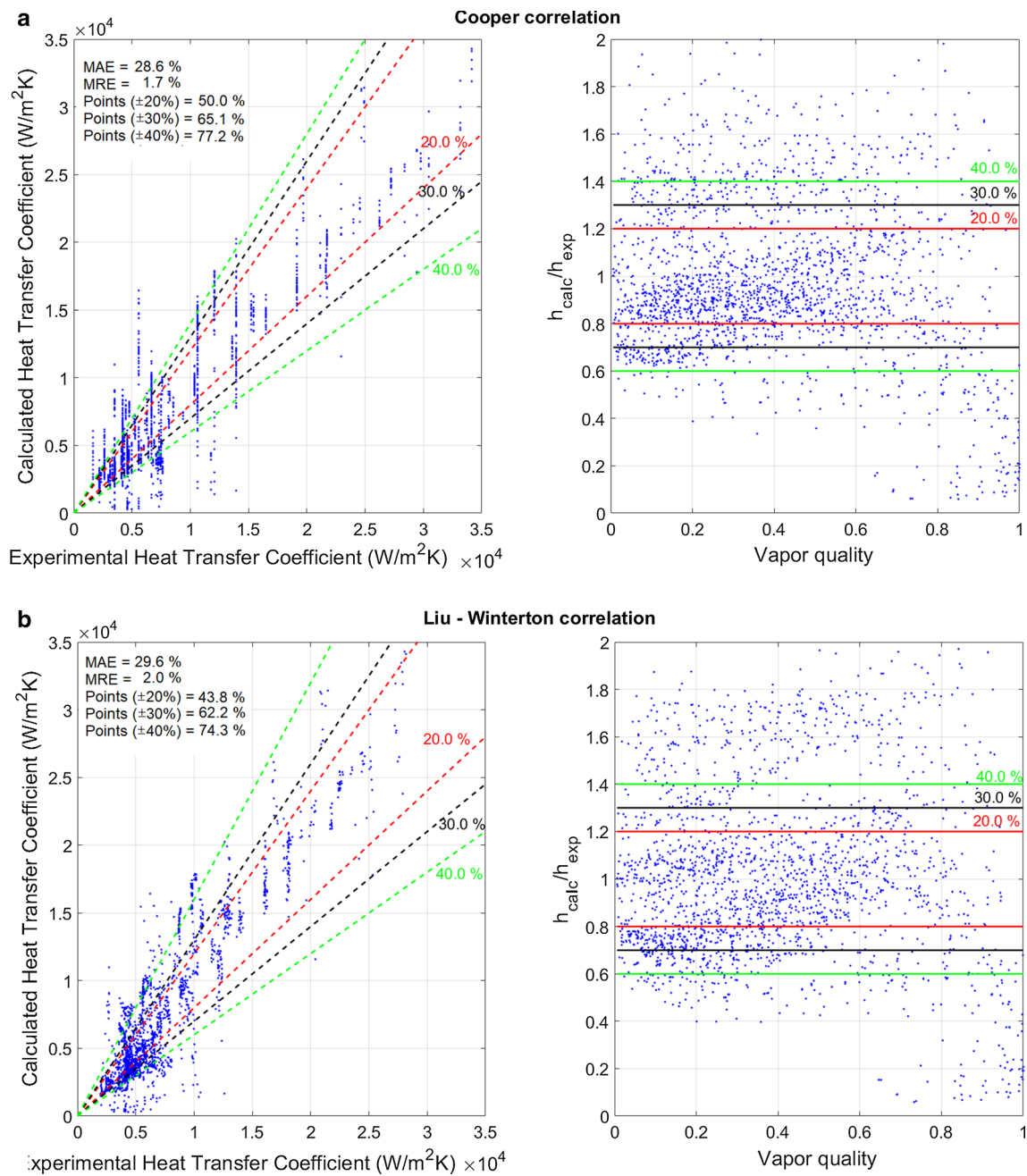
Fig. 4 Deviation analysis and prediction error distribution with increasing vapor qualities for **a** Cooper [41] and **b** Liu–Winterton [48] correlations

Relying on the numerical outcomes of extensive deviation analysis based on trial-and-error procedure, liquid Froude number is removed from the proposed model which is active in the flow boiling correlation of Wattelet et al. [49]. The model constants C_1–C_{14} are iteratively adjusted through Harris Hawks Optimization Algorithm [55] until the cumulative error between the experimental data and output of the proposed flow boiling model is minimized to its optimum value. A total number of 30 algorithm runs along with 50,000 maximum number of iterations have been performed. Harris Hawks' population is set to $N = 100$ for each algorithm run. Optimum solution with a minimum fitness value is considered as the global optimum solution, and respective design variables of the global optimum solution which are correlation constants
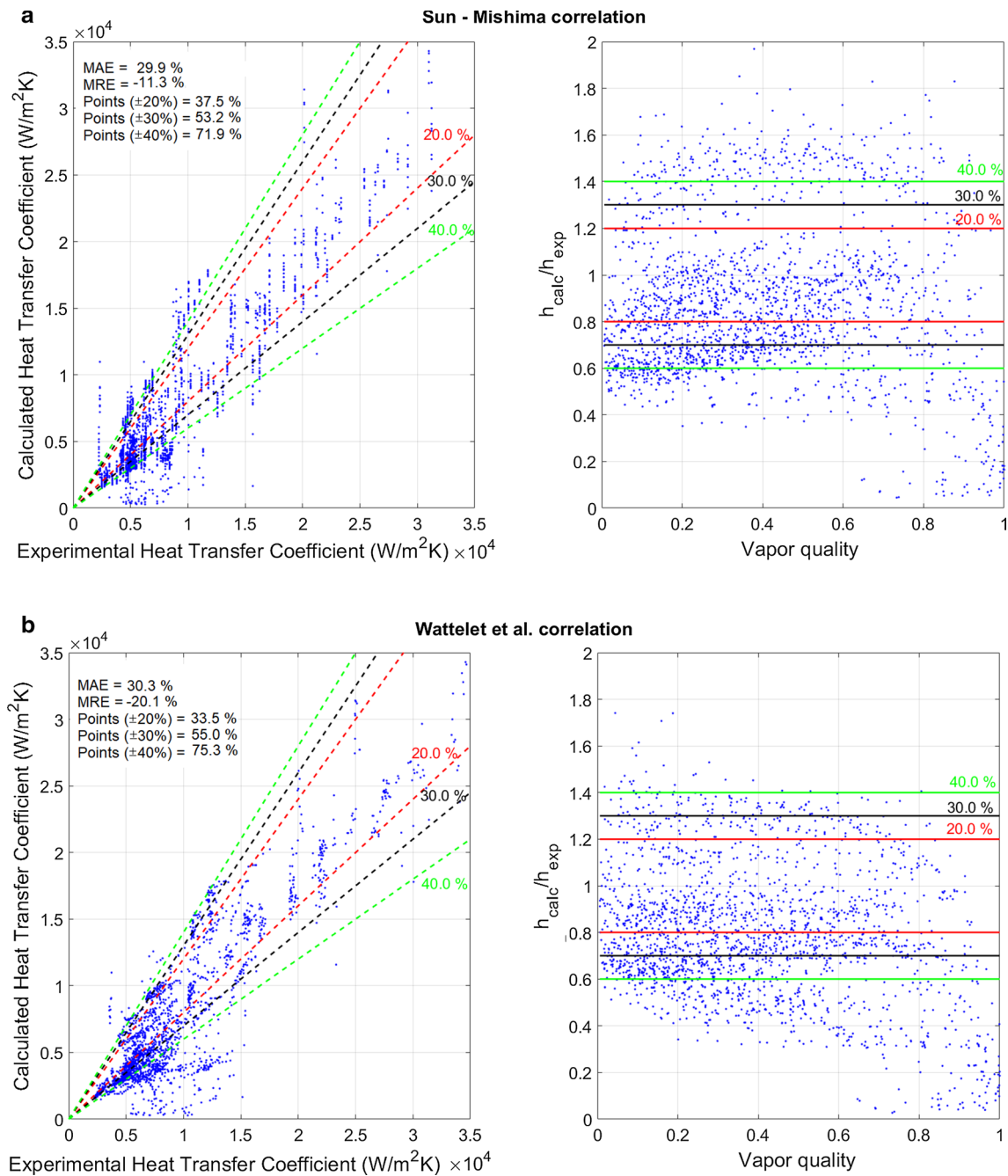
Fig. 5 Schematic representation of the prediction performances for correlations of **a** Sun–Mishima [43] and **b** Wattelet et al. [49]

C_1 to C_{14} of the proposed flow boiling model are reported in Table 11.

For the compiled propane flow boiling database consisting of 2179 points, the proposed flow boiling model has a MAE of 19.1% and MRE of − 2.9%, estimating 81.5% of the database within ± 30.0% and 92.8% of the database within ± 40.0% error bands, which are much better than those obtained by the compared literature flow boiling correlations. Apart from the proposed model, the second-best

existing correlation of Cooper [41] has a MAE of 28.6% and MRE of 1.7 predicting 65.1% of the experimental flow boiling data within 30.0% and 77.2% of the data within 40.0% error bands. Figure 7 depicts the prediction error distribution for the proposed flow boiling model. It is seen that deviation from the experimental data decreases with increasing vapor qualities which indicates that the trends of heat transfer coefficients obtained in the dry-out region

a

b
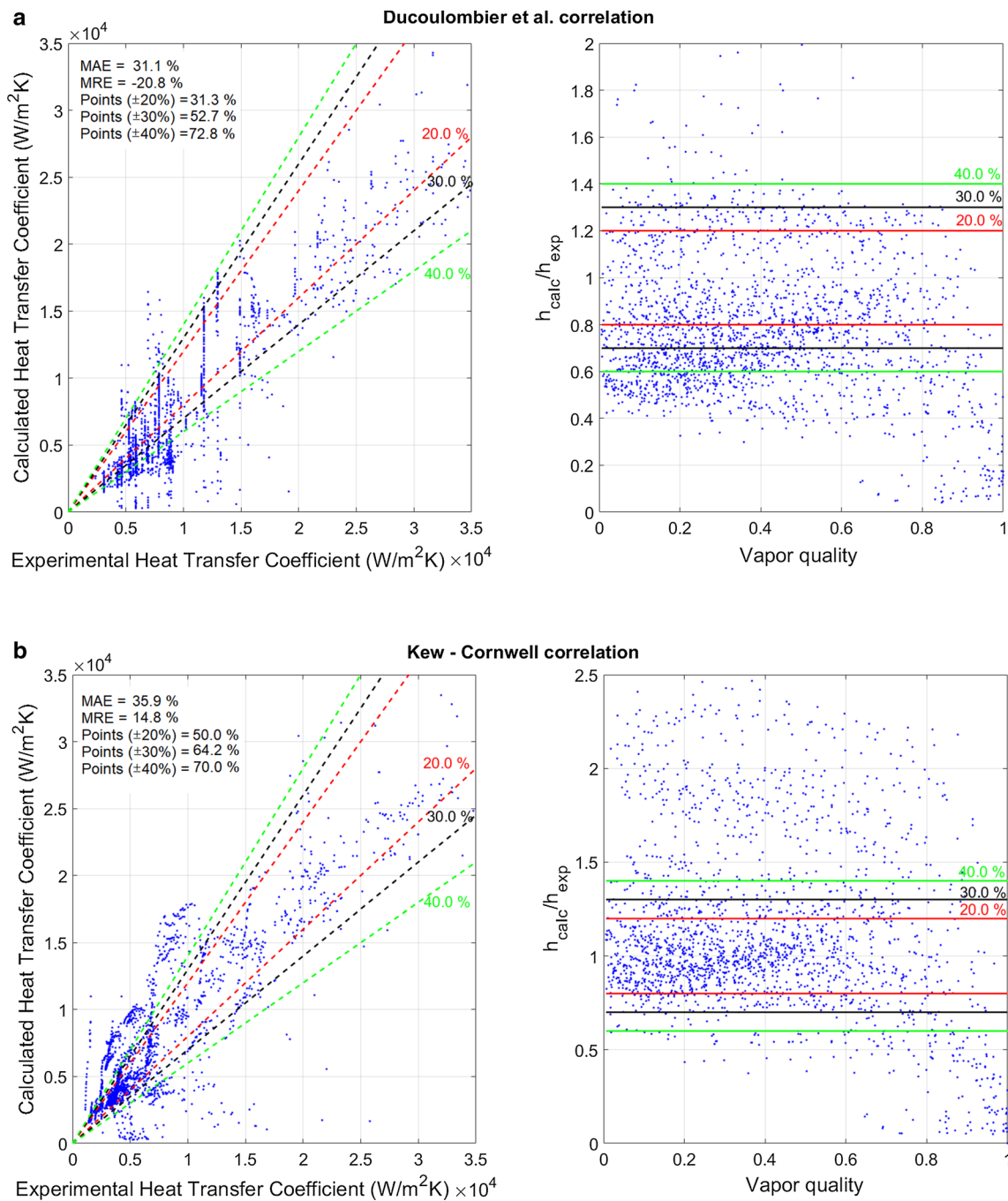
Fig. 6 Error distribution of the correlations of Ducoulombier et al. [52] and Kew–Cornwell [33] over the entire experimental database

can be accurately captured by the proposed model. Table 12 reports the deviation results of each experimental database retained from the proposed flow boiling model. The best predictive performance is shown for the database of Maqbool et al. [5] with a MAE of 7.0% and MRE of -3.3%, while the worst estimations are made for the experimental database obtained from Wang et al. [26] with a MAE of 34.4% and MRE of 31.9%. Figure 8 visualizes the comparison between the predictions performed by the proposed methods against

different experimental databases with different operational conditions. Well prediction of the experimental data is clearly observed as variational trends of the experimental heat transfer coefficients with increasing qualities are successfully captured by the proposed model with negligible discrepancies for each dataset. Figure 9a shows the variations of heat transfer coefficient values obtained from the proposed model along with the top six best performing flow boiling correlations of Cooper [41], Liu-Winterton [48], Sun

Table 11 Optimized correlation constants for the proposed flow boiling model

C_1	C_2	C_3	C_4
0.333782716243973	0.943831605461935	0.435826687089586	1.499118607477336
C_5	C_6	C_7	C_8
− 1.040878186584161	66.636181187049520	1.244926529779103	0.258952076070707
C_9	C_{10}	C_{11}	C_{12}
0.399836377153093	0.505546027893485	0.551669381417827	0.185318440184329
C_{13}		C_{14}	
0.354519104766204		2.695516415880346	
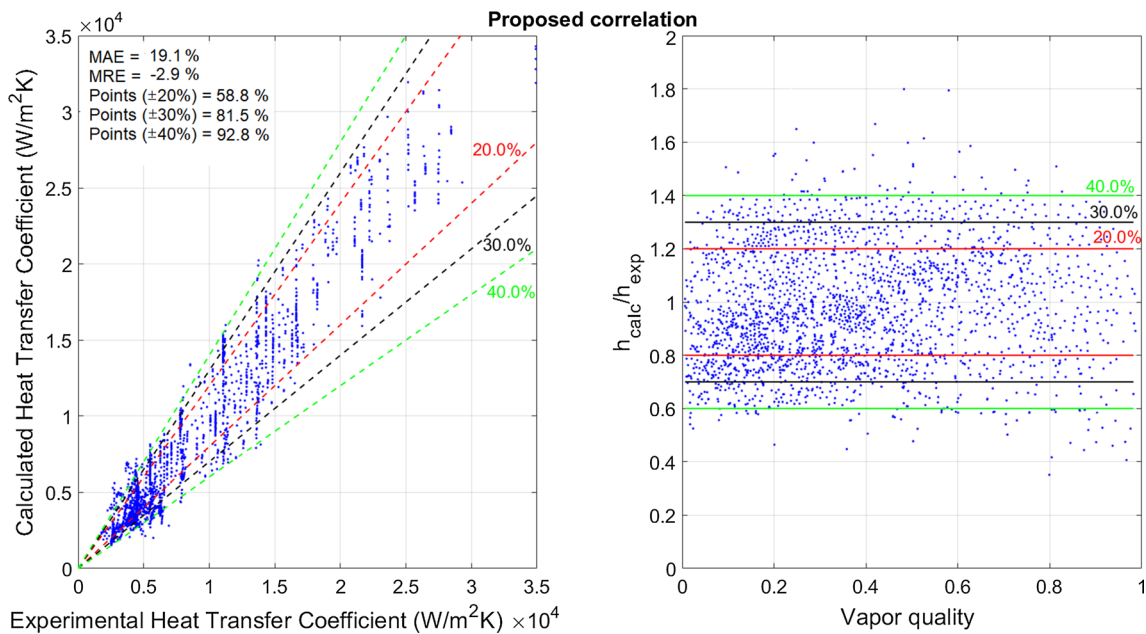
Fig. 7 Experimental versus calculated heat transfer coefficients along with normalized heat transfer coefficients with increasing vapor qualities for the proposed flow boiling model

Table 12 Deviation results of the proposed flow boiling model for each experimental database

	Anwar et al. [16]	Chien et al. [17]	Chien et al. [18]	Choi and Oh [19]	Citarella et al. [14]	Del col et al. [20]	Allymehr [21]	Lillo et al. [4]	Longo et al. [22]
MAE	10.7	22.2	28.2	14.5	18.2	12.5	34.0	21.1	21.8
MRE	− 5.6	− 21.9	− 0.1	− 9.2	17.8	− 3.2	− 33.9	20.0	20.1
	Maqbool et al. [5]	Maqbool et al. [23]	de Oliviera et al. [13]	Pamitran et al. [24]	Pamitran et al. [25]	Shin et al. [7]	Wang et al. [26]	Wang et al. [27]	Zhu et al. [28]
MAE	7.0	7.7	20.3	15.4	21.2	18.2	34.4	30.4	14.9
MRE	− 3.3	− 1.5	− 7.3	− 7.7	− 18.1	1.6	31.9	19.8	− 11.4

and Mishima [43], Wattelet et al. [49], Ducoulombier et al. [52], and Kew–Cornwell [33] for the operational conditions where $G = 200.0$ kg/m^{2}s, $D_h = 2.0$ mm, $T = 10.0$ °C, and $Q = 5.0$ kW/m^2. Experimental heat transfer rates gradually increase with increasing qualities, and most of the correlations obey this inclination of the experimental data, except for nucleate boiling-based modes which are independent of vapor quality. The proposed model has the capability to trace

a

Heat transfer coefficient (W/m²K) vs Vapor quality

Measured	Predicted	G (kg/m²s)	T (°C)	D (mm)	Q (kW/m²)
■	—	300.0	32.0	1.7	60.0
■	—	250.0	10.0	1.5	10.0
■	—	350.0	10.0	0.3	20.0
■	—	150.0	9.0	3.0	25.0
■	—	400.0	23.0	1.7	160.0

b

Heat transfer coefficient (W/m²K) vs Vapor quality

Measured	Predicted	G (kg/m²s)	D (mm)	T (°C)	Q (kW/m²)
■	—	200.0	2.0	5.0	10.0
■	—	400.0	1.7	23.0	80.0
■	—	300.0	1.7	33.0	100.0
■	—	400.0	0.96	40.0	75.0
■	—	300.0	6.0	25.0	20.0
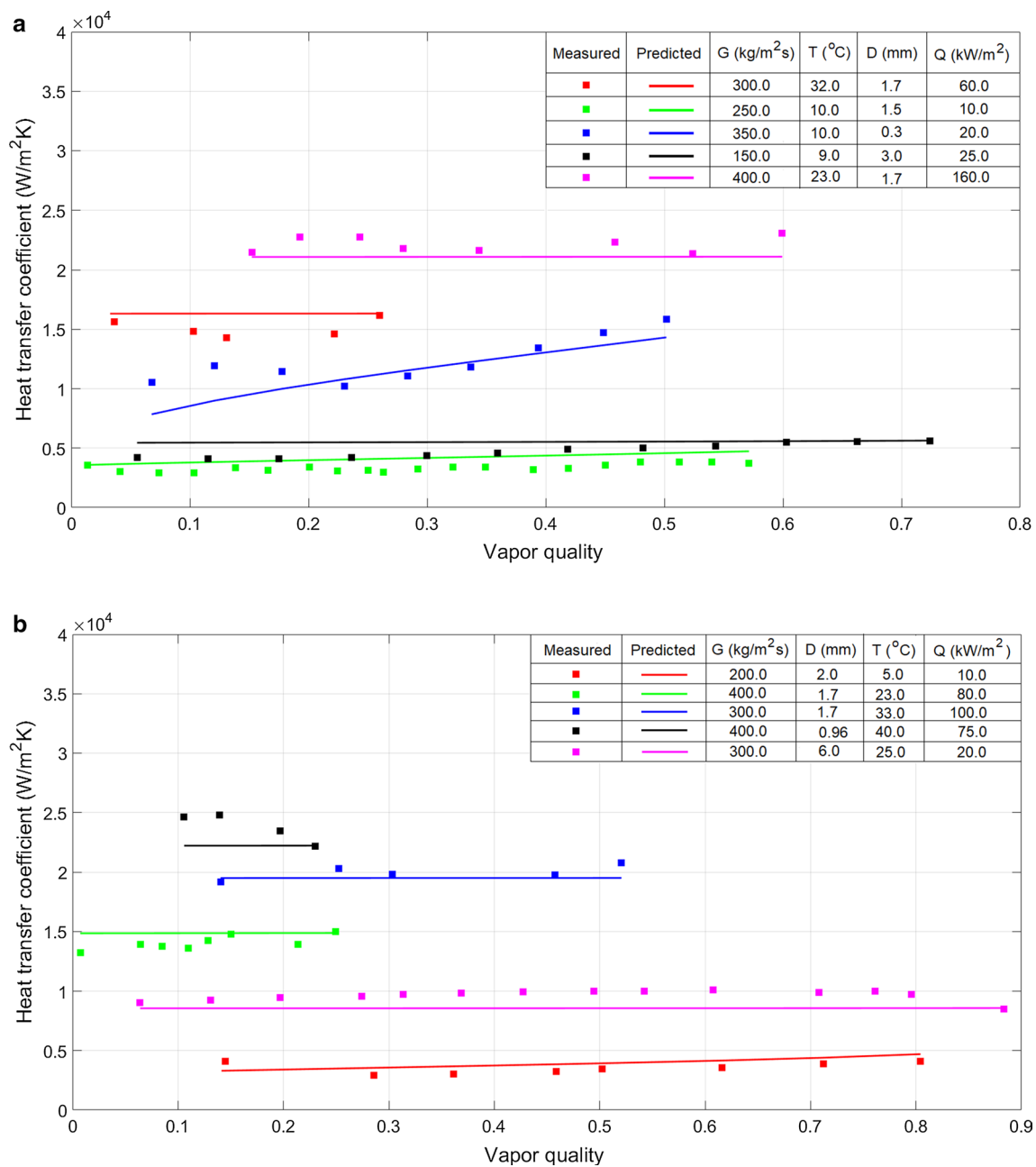
Fig. 8 Inclinations of the flow boiling heat transfer coefficients with increasing vapor quality: Experimental versus estimated data

the inclinations of the heat transfer coefficient experimental data with qualities. It is also seen those correlations of Wattelet et al. [49], and Ducoulombier et al. [52] considerably overpredict the actual data over the whole quality region. Estimation accuracy of the Cooper [41] correlation is satisfactory at lower qualities; however, predictive heat transfer coefficient rates deteriorate at higher qualities for this correlation. Underestimation of the actual data is observed for Kew–Cornwell [33] correlation, particularly at higher qualities. Correlation of Sun–Mishima [43] can capture the trends of experimental data, particularly at lower qualities. Figure 9b compares the predictions of the above-mentioned top six correlations accompanied by estimations of the flow boiling model for the experimental database obtained under the operational conditions of $G = 500.0$ kg/m²s, $D_h = 6.0$ mm, $T = 25.0$ °C, and $Q = 10.0$ kW/m². Correlations of Wattelet et al. [49] and Ducoulombier et al. [52] again significantly overestimates the experimental data over the entire quality region. Correlations of Cooper [41], and Kew–Cornwell [33] show underestimations of the actual data over the whole quality span. Predictions made by Liu–Winterton [48] are quite satisfactory at lower qualities;
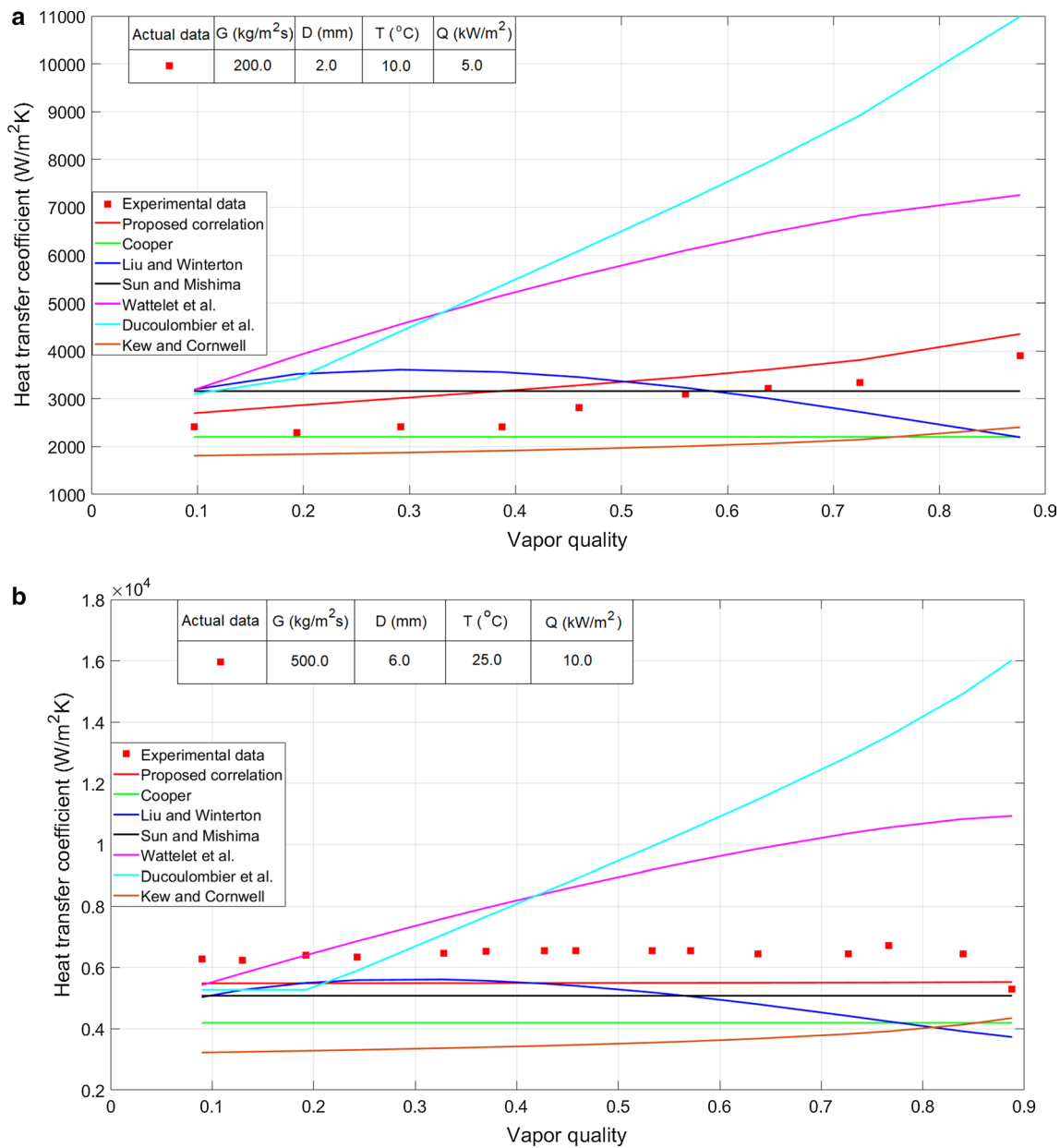
Fig. 9 Effects of thermodynamic qualities on heat transfer coefficient rates for different experimental databases

however, deviations grow bigger with increasing qualities. The new boiling model shows a strong ability to capture the inclinations of heat transfer coefficients and outperforms the compared correlations in terms of estimation accuracy.

Table 13 reports the prediction accuracy of the top three correlations including the new flow boiling model for different vapor quality regions. Huge deviations are observed in the high quality region for Chien et al. [17] and Pamitran et al. [25] databases for three best performing correlations, which suggest that dry-out effects play an important role on heat transfer coefficient rates. Inaccurate predictions shown by these models for these two databases also indicate that

the dry-out mechanism is not effectively modeled for these three correlations. It is also interesting to see that the new flow boiling model and the other two most successful correlation fail to estimate the heat transfer data of Allymehr [21], yielding relatively higher deviation results compared to the other databases. Correlations of Cooper et al. [41] and Liu–Winterton [48] are unable to predict the correct trends of the heat transfer coefficients in the dry-out zones of the experimental database of Chien et al. [17], Choi and Oh [19], Citarella et al. [14], Lillo et al. [4], de Oliviera et al. [13], Pamitran et al. [24], and Zhu et al. [28]. One can see that estimating the dry-out heat transfer coefficients is

Table 13 Deviation results of top three flow boiling correlation for different vapor quality bands

		New model		Cooper [41]		Liu–Winterton [48]	
		MAE	MRE	MAE	MRE	MAE	MRE
Anwar et al. [16]	(0.0,0.3)	13.0	9.8	9.7	8.4	10.2	9.4
	(0.3,0.7)	10.6	5.1	9.5	7.4	10.2	9.4
	(0.7,1.0)	10.0	10.0	2.5	2.5	3.5	3.5
Chien et al. [17]	(0.0,0.3)	24.4	24.4	15.1	14.4	57.9	57.9
	(0.3,0.7)	34.2	33.6	44.5	39.8	176.6	176.6
	(0.7,1.0)	108.9	108.9	442.7	442.7	994.4	994.4
Chien et al. [18]	(0.0,0.3)	27.5	9.8	33.2	− 7.3	52.6	27.5
	(0.3,0.7)	24.3	15.0	57.1	12.6	129.9	112.1
	(0.7,1.0)	9.9	9.9	430.0	367.4	835.4	807.8
Choi and Oh [19]	(0.0,0.3)	29.9	29.9	47.4	47.4	56.2	56.2
	(0.3,0.7)	10.1	2.9	18.8	14.4	36.4	36.4
	(0.7,1.0)	6.3	− 6.2	160.3	155.6	223.1	223.1
Citarella et al. [14]	(0.0,0.3)	18.2	17.8	25.9	− 25.9	22.0	− 22.0
	(0.3,0.7)	12.4	− 12.4	29.0	− 29.0	17.8	− 17.8
	(0.7,1.0)	16.6	− 16.6	82.9	53.3	92.4	83.9
Del col et al. [20]	(0.0,0.3)	11.1	2.2	15.9	− 15.9	14.1	− 14.0
	(0.3,0.7)	61.8	61.8	15.0	15.0	18.3	18.3
	(0.7,1.0)	N/A	N/A	N/A	N/A	N/A	N/A
Allymehr [21]	(0.0,0.3)	70.5	70.5	108.0	108.0	150.2	150.2
	(0.3,0.7)	55.6	55.6	90.9	90.9	172.1	172.1
	(0.7,1.0)	49.9	49.7	169.6	169.6	295.0	295.0
Lillo et al. [4]	(0.0,0.3)	14.5	− 13.9	32.5	− 32.5	23.9	− 21.7
	(0.3,0.7)	17.5	− 17.0	34.2	− 34.2	19.2	− 17.7
	(0.7,1.0)	16.3	− 10.9	88.4	53.3	95.9	85.6
Longo et al. [22]	(0.0,0.3)	15.0	− 13.6	8.0	− 7.6	3.1	1.8
	(0.3,0.7)	18.3	− 16.4	13.1	− 12.5	5.6	4.9
	(0.7,1.0)	9.2	− 6.8	14.1	− 13.5	4.9	4.9
Maqbool et al. [5]	(0.0,0.3)	8.5	7.2	11.4	10.9	12.9	12.6
	(0.3,0.7)	5.7	0.7	10.6	9.2	12.5	11.2
	(0.7,1.0)	10.2	3.9	26.6	18.0	28.6	20.1
Maqbool et al. [23]	(0.0,0.3)	8.4	5.3	12.7	12.5	14.5	14.5
	(0.3,0.7)	6.8	− 4.0	12.6	12.2	14.8	14.5
	(0.7,1.0)	9.9	6.7	38.3	38.3	41.3	41.3
de Oliviera et al. [13]	(0.0,0.3)	24.8	12.2	23.3	− 7.6	29.6	23.6
	(0.3,0.7)	24.1	17.7	18.9	− 2.3	48.5	46.6
	(0.7,1.0)	30.0	30.0	86.6	86.6	109.4	109.4
Pamitran et al. [24]	(0.0,0.3)	27.3	27.3	44.3	44.3	57.9	57.9
	(0.3,0.7)	11.6	0.6	13.5	7.7	37.3	37.3
	(0.7,1.0)	12.8	− 7.9	408.1	408.1	566.0	566.0
Pamitran et al. [25]	(0.0,0.3)	33.9	33.1	25.6	22.9	55.7	55.7
	(0.3,0.7)	21.1	15.7	17.4	10.9	57.2	57.2
	(0.7,1.0)	61.8	60.1	434.1	433.9	781.5	781.5
Shin et al. [7]	(0.0,0.3)	21.1	20.3	37.5	37.5	58.9	58.9
	(0.3,0.7)	15.9	− 12.7	10.7	− 0.1	36.0	36.0
	(0.7,1.0)	N/A	N/A	N/A	N/A	N/A	N/A
Wang et al. [26]	(0.0,0.3)	34.2	− 34.2	19.3	19.3	24.0	24.0
	(0.3,0.7)	19.4	− 18.9	14.9	14.9	29.5	29.5
	(0.7,1.0)	20.2	− 6.5	15.1	15.1	36.2	36.2
Wang et al. [27]	(0.0,0.3)	22.6	− 17.3	25.1	25.1	31.0	31.0

Table 13 (continued)

		New model		Cooper [41]		Liu–Winterton [48]	
		MAE	MRE	MAE	MRE	MAE	MRE
	(0.3,0.7)	23.3	− 11.9	22.3	17.4	33.5	33.5
	(0.7,1.0)	29.8	3.8	24.9	20.4	42.4	42.4
Zhu et al. [28]	(0.0,0.3)	19.9	19.9	14.3	11.3	66.9	66.9
	(0.3,0.7)	15.0	10.5	14.1	− 9.0	85.9	85.9
	(0.7,1.0)	20.9	16.6	164.8	141.1	475.4	475.4

extremely difficult, and Fang et al. [56] reported that energy error in the order of 2.0–3.0% in the experiments may yield up to 40.0% errors in flow regimes and dry out inception qualities. Extensive theoretical evaluations on flow boiling models reveal that although flow pattern-based flow boiling correlations of Thome and El Hajal [57] and Saitoh et al. [58] have a criterion for dry-out inception, their estimation accuracy for the dry-out zone is still in quandary and they are not capable of yielding satisfactory predictions for this flow regime. This can be attributed to the fact that each refrigerant has intrinsic thermal properties and a general dry out incipience correlation developed for a particular refrigerant may not be suitable for any other refrigerant, which results in erroneous predictions in general applications. Therefore, utmost care should be given when modeling a flow boiling correlation to this flow region. Furthermore, refrigerant specific dry-out inception correlations should be developed if it is to obtain more reliable predictions regarding the mist flow regime heat transfer coefficients.

6 Conclusion

Based on 2179 experimental data of propane obtained from eighteen different laboratories around the world, a new two-phase flow boiling heat transfer model is developed which is a modified version of Wattelet et al. [49] correlation. Compiled flow boiling experimental data of propone cover mass flux from 50 to 600 kg/m^{2}s, saturation temperature from -35.0 to 43.0 °C, heat flux from 2.5 to 227.0 kW/m^2, hydraulic diameter 0.3 to 7.7 mm, and vapor quality 0.01 to 0.99. A new flow boiling model agrees well for most of the dataset with having a MAE of 19.1% and MRE of 1.7%. The proposed model predicts 81.5% of the whole accumulated experimental database within $\pm$ 30.0 error zone and 92.8% within the 40.0% error zone. Estimation accuracy of the proposed model is benchmarked against some of the well-reputed literature flow boiling correlations with different structural forms. The main purpose of using the propane

database is to develop better than the existing literature flow boiling correlations whose prediction performances for propane refrigerant are not satisfactory enough to be used for a wide range of operational conditions. These correlations do not perform well for the propane refrigerant because they are not developed for the propane or they are developed for specific operational ranges of propane.

After a detailed investigation on the tendencies of the compiled measured flow boiling heat transfer coefficients of propane with varying operational parameters including mass flux, heat flux and vapor quality, the following insightful deductions can be drawn:

- Local flow boiling heat transfer coefficients increase with increasing vapor qualities until the occurrence of the dry-out, and then gradual decreases are observed as given in Fig. 3b.
- Increasing mass fluxes and heat fluxes increases the flow boiling heat transfer coefficient rates.

Between three vapor quality zones, the most deviated predictions are obtained for the quality range which is under the effect of dry out conditions. Comprehending the influences of the dry-out mechanism on the inclinations of heat transfer coefficients becomes the utmost challenge for practitioners and researchers working on this subject. A better understanding of this hot spot research subject will yield more accurate and reliable flow boiling correlations. Major limitation of these types of flow boiling models is that their prediction accuracies deteriorate if operational parameters exceed the restricted ranges of experimental conditions in which the flow boiling model is correlated for. Future studies on this research subject should focus on developing refrigerant-specific flow boiling models based on the measured experimental data covering a wide range of operational conditions. Flow boiling models developed under these circumstances not only tend to provide more reliable predictions but also eliminate the exhaustive process of finding a suitable flow boiling model for the related refrigerant.

References

1. Sardeshpande, M.; Ranade, V.V.: Two-phase flow boiling in small channels: a brief review. Sadhana **38**, 1083–1125 (2013). https://doi.org/10.1007/s12046-013-0192-7

2. Fang, X.; Zhuang, F.; Chen, C.; Wu, Q.; Chen, Y.; Chen, Y.; He, Y.: Saturated flow boiling heat transfer: review and assessment of prediction methods. Heat Mass Transf. **5**, 197–222 (2019). https://doi.org/10.1007/s00231-018-2432-1

3. Gao, Y.; Shao, S.; Zhan, B.; Chen, Y.; Tian, C.: Heat transfer and pressure drop characteristics of ammonia during flow boiling inside a horizontal small diameter tube. Int. J. Heat Mass Transf. **127**, 981–996 (2018). https://doi.org/10.1016/j.ijheatmasstransfer.2018.07.137

4. Lillo, G.; Mastrullo, R.; Mauro, A.W.; Viscito, L.: Flow boiling heat transfer, dry-out vapor quality and pressure drop of propane (R290): experimental and assessment of predictive methods. Int. J. Heat Mass Transf. **126**, 1236–1252 (2018). https://doi.org/10.1016/j.ijheatmasstransfer.2018.06.069

5. Maqbool, M.M.; Palm, B.; Khodabandeh, R.: Investigation of two-phase heat transfer and pressure drop of propane in a vertical circular minichannel. Exp. Therm. Fluid Sci. **46**, 120–130 (2013). https://doi.org/10.1016/j.expthermflusci.2012.12.002

6. James, R.W.; Missenden, J.F.: The use of propane in domestic refrigerators Int. J. Refrig. **15**, 95–100 (1992). https://doi.org/10.1016/0140-7007(92)90033-Q

7. Shin, J.Y.; Kim, M.S.; Ro, S.T.: Experimental study on forced convective boiling heat transfer of pure refrigerants and refrigerant mixtures in a horizontal tube. Int. J. Refrig. **20**, 267–275 (1997). https://doi.org/10.1016/S0140-7007(97)00004-2

8. Gungor, K.E.; Winterton, R.H.S.: Simplified general correlation for saturated flow boiling and comparisons of correlations with data. Chem. Eng. Res. Des. **65**, 148–156 (1987)

9. Lee, H.S.; Yoon, J.I.; Kim, J.D.; Bansal, P.: Evaporating heat transfer and pressure drop of hydrocarbon refrigerants in 9.52- and 12.70-mm smooth tube. Int. J. Heat Mass Transf. **48**, 2351–2359 (2005). https://doi.org/10.1016/j.ijheatmasstransfer.2005.01.012

10. Wen, M.Y.; Ho, C.Y.: Evaporation heat transfer and pressure drop characteristics of R290 (propane), R600 (butane), and a mixture of R-290/R-600 in three lines serpentine small tube bank. Appl. Therm. Eng. **25**, 2921–2936 (2005). https://doi.org/10.1016/j.applthermaleng.2005.02.013

11. Zou, X.; Gong, M.; Chen, G.; Sun, Z.; Wu, J.: Experimental study on saturated flow boiling heat transfer of R290/R152a binary mixtures in a horizontal tube. Front. Energ. Power Eng. China **4**, 527–534 (2010). https://doi.org/10.1007/s11708-010-0109-7

12. Yunos, Y.M.; Ghazali, N.M.; Pamitran, A.S.; Novianto, S.: Analysis of the Two-phase heat transfer coefficient of propane in small channel. Energy Procedia **105**, 4635–4640 (2017). https://doi.org/10.1016/j.egypro.2017.03.1004

13. de Oliveira, J.D.; Passos, J.C.; Copetti, J.B.; van der Geld, C.W.M.: Flow boiling heat transfer of propane in 1.0 mm tube. Exp. Therm. Fluid. Sci. **96**, 243–256 (2018). https://doi.org/10.1016/j.expthermflusci.2018.03.010

14. Citarella, B.; Lillo, G.; Mastrullo, R.; Mauro, A.W.; Viscito, L.: Experimental investigation on flow boiling heat transfer and pressure drop of refrigerants R32 and R290 in a stainless-steel horizontal tube. J. Phys. Conf. Ser. **1224**, 012041 (2019). https://doi.org/10.1088/1742-6596/1224/1/012041

15. Kandlikar, S.G.: Fundamental issues related to flow boiling in minichannel and microchannels. Exp. Therm. Fluid Sci. **26**, 38–47 (2002). https://doi.org/10.1016/S0894-1777(02)00150-4

16. Anwar, Z.; Ahmed, I.; Noor, F.; Ali, Z.; Imran, S.; Siyal, S.H.; Sultan, T.: Flow boiling heat transfer characteristics of R600A and R290 in vertical mini-channels. JFET **21**, 164–181 (2014)

17. Chien, N.B.; Vu, P.Q.; Choid, K.I.; Oh, J.T.: Boiling heat transfer of R32, CO_2 and R290 inside Horizontal Minichannel. Energy Procedia **105**, 4822–4827 (2017). https://doi.org/10.1016/j.egypro.2017.03.955

18. Chien, N.B.; Vu, P.Q; Choi, K.I.; Oh, J.T.: An experimental investigation of convective boiling heat transfer using alternative and natural refrigerants inside horizontal microchannels. In: International Refrigeration and Air Conditioning Conference, Paper 1669 (2016)

19. Choi, K.I.; Oh, J.T.: Characteristics of two-phase flow boiling heat transfer of NH_3, C_3H_8 and CO_2 in horizontal circular small tubes. In: 7th International Conference on Heat Transfer, Fluid Mechanics and Thermodynamics, 19–21 July, Antalya, Turkey (2010)

20. Del Col, D.; Bortolato, M.; Bortolin, S.: Comprehensive experimental investigation of two-phase heat transfer and pressure drop with propane in a minichannel. Int. J. Refrig. **47**, 66–84 (2014). https://doi.org/10.1016/j.ijrefrig.2014.08.002

21. Allymehr, E. Experimental investigation of EVAPORATION of Propane (R290) in Small Pipes, Master Thesis, Politecnico Di Milano, Italy (2017)

22. Longo, G.A.; Mancin, S.; Righetti, G.; Zilio, C.: Hydrocarbon refrigerants HC290(Propane) and HC1270(Propylene) low GWP long-term substitutes for HFC404A: a comparative analysis in vaporization inside a small-diameter horizontal smooth tube. Appl. Therm. Eng. **124**, 707–715 (2017). https://doi.org/10.1016/j.applthermaleng.2017.06.080

23. Maqbool, M.H.; Palm, B.; Khodabandeh, R.; Ali, R.R.: Saturated flow boiling heat transfer characteristics of propane in a smooth vertical minichannel up to dryout incipience. In: 23rd IIR Congress of Refrigeration, Prague, Czech Republic, 21–26 August, 2011

24. Pamitran, A.S.; Choi, K.I.; Oh, J.T.; Park, K.W.: Two-phase flow heat transfer of propane vaporization in horizontal minichannels. J. Mech. Sci. Technol. **23**, 599–606 (2009). https://doi.org/10.1007/s12206-008-0913-8

25. Pamitran, A.S.; Choi, K.I.; Oh, J.T.: Nasruddin: evaporation heat transfer coefficient in single circular small tubes for flow natural refrigerants of C_3H_8, NH_3 and CO_2. Int. J. Multiph. Flow **37**, 794–801 (2011). https://doi.org/10.1016/j.ijmultiphaseflow.2011.02.005

26. Wang, S.; Gong, M.; Chen, G.; Wu, J.; Sun, Z.; Zou, X.: Two-phase flow boiling heat transfer characteristic of propane in a smooth horizontal tube. In: Proceedings of 24th International Cryogenic Engineering Conference and International Cryogenic Materials Conference, Fukuoka, Japan, 14–18 May, 2012

27. Wang, S.; Gong, M.Q.; Chen, G.F.; Sun, Z.H.; Wu, J.F.: Two-phase heat transfer and pressure drop of propane during saturated flow boiling inside a horizontal tube. Int. J. Refrig. **41**, 200–209 (2014). https://doi.org/10.1016/j.ijrefrig.2013.03.019

28. Zhu, Y.; Wu, X.; Wei, Z.: Heat transfer characteristics and correlation for CO_2/propane mixtures flow evaporation in a smooth mini tube. Appl. Therm. Eng. **81**, 253–261 (2015). https://doi.org/10.1016/j.applthermaleng.2015.02.009

29. Dougall, R.S.; Rohsenow, W.M.: Film Boiling on the Inside of Vertical Tubes with Upward Flow of the Fluid at Low Qualities. MIT Report No.9079-26 (1963)

30. Groeneveld, D.C.: An Investigation of Heat Transfer in the Liquid Deficient Regime. Report AECL-3281 (1969)

31. Dittus, F.W.; Boelter, L.M.K.: Heat transfer in automobile radiators of the tubular type. Int. Commun. Heat Mass Transf. **12**, 3–22 (1985). https://doi.org/10.1016/0735-1933(85)90003-X

32. Kenning, D.B.R.; Cooper, M.G.: Saturated flow boiling of water in vertical tubes. Int. J. Heat Mass Transf. **32**, 445–458 (1989). https://doi.org/10.1016/0017-9310(89)90132-4

33. Kew, P.A.; Cornwell, K.: Correlations for prediction of boiling heat transfer in small-diameter channels. Appl. Therm. Eng. **17**, 705–715 (1997). https://doi.org/10.1016/S1359-4311(96)00071-3

34. Li, W.; Wu, Z.: A general correlation for evaporative heat transfer in micro/mini channels. Int. J. Heat Mass Transf. **53**, 1778–1787 (2010). https://doi.org/10.1016/j.ijheatmasstransfer.2010.01.012

35. Yan, Y.Y.; Lin, T.F.: Evaporation heat transfer and pressure drop of refrigerant R-134a in a small pipe. Int. J. Heat Mass Transf. **41**, 4183–4194 (1998). https://doi.org/10.1016/S0017-9310(98)00127-6

36. Chen, J.C.: Correlation for boiling heat transfer to saturated fluids in convective flow. I&EC Process. Des. Dev. **5**, 322–329 (1966). https://doi.org/10.1021/i260019a023

37. Gungor, K.E.; Winterton, R.H.S.: General correlation for flow boiling in tubes and annuli. Int. J. Heat Mass Transf. **26**, 351–358 (1986). https://doi.org/10.1016/0017-9310(86)90205-X

38. Jung, D.S.; McLinden, M.; Radermacher, R.; Didion, D.: A study of flow boiling heat transfer with refrigerant mixtures. Int. J. Heat Mass Transf. **32**, 1751–1764 (1989). https://doi.org/10.1016/0017-9310(89)90057-4

39. Choi, K.I.; Pamitran, A.S.; Oh, J.T.: Two-phase flow heat transfer of CO_2 vaporization in smooth horizontal mini channels. Int. J. Refrig. **30**, 767–777 (2016). https://doi.org/10.1016/j.ijrefrig.2006.12.006

40. Mahmoud, M.M.; Karayiannis, T.G.: Heat transfer correlation for flow boiling in small to micro tubes. Int. J. Heat Mass Transf. **66**, 553–574 (2013). https://doi.org/10.1016/j.ijheatmasstransfer.2013.07.042

41. Cooper, M.G.: Heat flow rates in saturated nucleate pool boiling—a wide ranging examination using reduced properties. Adv. Heat. Trans. **16**, 157–239 (1984). https://doi.org/10.1016/S0065-2717(08)70205-3

42. Stephan, K.; Abdelselam, M.: Heat transfer correlations for natural convection boiling. Int. J. Heat Mass Transf. **23**, 73–87 (1980). https://doi.org/10.1016/0017-9310(80)90140-4

43. Sun, L.; Mishima, K.: An evaluation of prediction methods for saturated flow boiling heat transfer in mini-channels. Int. J. Heat Mass Transf. **52**, 5323–5329 (2009). https://doi.org/10.1016/j.ijheatmasstransfer.2009.06.041

44. Lazarek, G.M.; Black, S.H.: Evaporative heat transfer, pressure drop and critical heat flux in a small vertical tube with R-113. Int. J. Heat Mass Transf. **25**, 945–959 (1982). https://doi.org/10.1016/0017-9310(82)90070-9

45. Hamdar, M.; Zoughaib, A.; Clodic, D.: Flow boiling heat transfer and pressure drop of pure HFC-152a in a horizontal mini-channel. Int. J. Refrig. **33**, 566–577 (2010). https://doi.org/10.1016/j.ijrefrig.2009.12.006

46. Tran, T.; Wambsganss, M.W.; France, D.M.: Small circular- and rectangular channel boiling with two refrigerants. Int. J. Multiphas. Flow **22**, 485–498 (1996). https://doi.org/10.1016/0301-9322(96)00002-X

47. Yu, W.; France, D.M.; Wambsganss, M.W.; Hull, J.R.: Two phase pressure drop, boiling heat transfer and critical heat flux to water in a small diameter horizontal tube. Int. J. Multiphas. Flow **28**, 927–941 (2002). https://doi.org/10.1016/S0301-9322(02)00019-8

48. Liu, Z.; Winterton, R.H.S.: A general correlation for saturated and subcooled flow boiling in tubes and annuli based on a nucleate pool boiling equation. Int. J. Heat Mass Transf. **34**, 2759–2766 (1991). https://doi.org/10.1016/0017-9310(91)90234-6

49. Wattelet, J.P.; Chato, J.C.; Souza, A.L.; Christoffersen, B.R.: Evaporative characteristics of R-12, R134a, and a mixture at low mass fluxes. ASHRAE Trans. **100**, 603–615 (1994)

50. Shah, M.M.: Chart correlation for saturated boiling heat transfer: equation and further study. ASHRAE Trans. **88**, 185–196 (1982)

51. Kandlikar, S.G.: A general correlation for two phase flow boiling heat transfer inside horizontal and vertical tubes. J. Heat Transf. **112**, 219–228 (1990). https://doi.org/10.1115/1.2910348

52. Ducoulombier, M.; Colasson, S.; Bonjour, J.; Haberschill, P.: Carbon dioxide flow boiling in a single microchannel—part II: heat transfer. Exp. Therm. Fluid Sci. **35**, 597–611 (2011). https://doi.org/10.1016/j.expthermflusci.2010.11.014

53. Lemmon, E.W.; McLinden, M.O.; Huber, M.L.: REFPROP, NIST Standard Reference Database 23, Version 7.1. (2013)

54. Fang, X.; Zhou, Z.; Wang, H.: Heat transfer correlation for saturated flow boiling of water. Appl. Therm. Eng. **76**, 147–156 (2015). https://doi.org/10.1016/j.applthermaleng.2014.11.024

55. Heidari, A.A.; Mirjalili, S.; Faris, H.; Aljarah, I.; Mafarja, M.; Chen, H.: Harris hawks optimization: algorithm and applications. Future Gener. Comput. Syst. **97**, 849–872 (2019). https://doi.org/10.1016/j.future.2019.02.028

56. Fang, X.; Zhou, Z.; Li, D.: Review of correlations of flow boiling heat transfer coefficients for carbon-dioxide. Int. J. Refrig. **36**, 2017–2039 (2013). https://doi.org/10.1016/j.ijrefrig.2013.05.015

57. Thome, J.R.; El Hajal, J.: Flow boiling heat transfer to carbon dioxide: general prediction method. Int. J. Refrig. **28**, 294–301 (2004). https://doi.org/10.1016/j.ijrefrig.2003.08.003

58. Saitoh, S.; Diaguji, H.; Hihara, E.: Correlation for boiling heat transfer of R134a in horizontal tubes including the effect of tube diameter. Int. J. Heat Mass Transf. **50**, 5215–5225 (2007). https://doi.org/10.1016/j.ijheatmasstransfer.2007.06.019